Ab Initio Anharmonic Analysis of Vibrational Spectra of Uracil Using the Numerical−Analytic Implementation of Operator Van Vleck Perturbation Theory

ARTICLE *in* THE JOURNAL OF PHYSICAL CHEMISTRY A · MAY 2015

Impact Factor: 2.69 · DOI: 10.1021/acs.jpca.5b03241 · Source: PubMed

3 AUTHORS, INCLUDING:

Sergey Krasnoshchekov
Lomonosov Moscow State University
38 PUBLICATIONS **473** CITATIONS

THE JOURNAL OF PHYSICAL CHEMISTRY A

Article

pubs.acs.org/JPCA

Ab Initio Anharmonic Analysis of Vibrational Spectra of Uracil Using the Numerical-Analytic Implementation of Operator Van Vleck Perturbation Theory

Sergey V. Krasnoshchekov,*[,†,‡] Natalja Vogt,[†,‡] and Nikolay F. Stepanov[†]

[†]Lomonosov Moscow State University, Leninskiye Gory, 119991, Moscow, Russian Federation

[‡]Chemieinformationssysteme, Universität Ulm, Albert Einstein Allee 47, D-89069 Ulm, Germany

Supporting Information

ABSTRACT: The numerical-analytic implementation of the operator version of the canonical Van Vleck second-order vibrational perturbation theory (CVPT2) is employed for a purely *ab initio* prediction and interpretation of the infrared (IR) and Raman anharmonic spectra of a medium-size molecule of the diketo tautomer of uracil (2,4(1*H*,3*H*)-pyrimidinedione), which has high biological importance as one of the four RNA nucleobases. A nonempirical, semidiagonal quartic potential energy surface (PES) expressed in normal coordinates was evaluated at the MP2/cc-pVTZ level of theory. The quality of the PES was improved by replacing the harmonic frequencies with the "best" estimated CCSD(T)-based values taken from the literature. The theoretical method is enhanced by an accurate treatment of multiple Fermi and Darling–Dennison resonances with evaluation of the corresponding resonance constants *W* and *K* (CVPT2+*WK* method). A prediction of the anharmonic frequencies as well as IR and Raman intensities was used for a detailed interpretation of the experimental spectra of uracil. Very good agreement between predicted and observed vibrational frequencies has been achieved (RMSD ~4.5 cm^{-1}). The model employed gave a theoretically robust treatment of the multiple resonances in the 1680–1790 cm^{-1} region. Our new analysis gives the most reliable reassignments of IR and Raman spectra of uracil available to date.

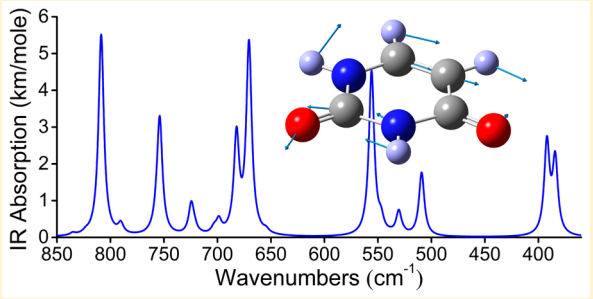

1. INTRODUCTION

One of the major goals of quantum mechanics (QM) and computational chemistry is an accurate modeling of physical-chemical phenomena that take place, for instance, in vibrational molecular spectroscopy, the field of our major interest. This modeling assists in verifying the adequacy of the theoretical concepts and the approximations employed in solving applied chemical problems such as spectral identification of various forms of molecules. The progress of computational vibrational spectroscopy rests upon theoretical and practical advances in solving the QM electronic problem, yielding potential energy surfaces (PES) and other molecular property surfaces (MPS), as well as theoretical descriptions of nuclear motion. A burst of fine achievements in the field of theoretical molecular spectroscopy is taking place today, as high QM accuracy in evaluation of PES and MPS is being combined with variational methods for smaller molecules or with the power of vibrational perturbation theory applied to molecules of larger size.[1]

The aim of the present study is 2-fold. First, we are making our target a state-of-the-art interpretation of the many published experimental vibrational spectra of uracil. We rely on purely *ab initio* methods without any fitting or scaling of data. Second, we want to demonstrate that an accurate implementation of the vibrational perturbation theory enables interpretation of most spectral features by direct comparison of peak positions and intensities in the infrared (IR) and Raman scattering (RS) spectra. Success of this approach may set a new standard in the theoretical modeling of spectra and avoid a number of well-known difficulties, such as synthesizing isotopically substituted molecules, analyzing isotopic shifts, choosing a nonredundant set of (locally) symmetrized internal coordinates, assembling reliable scale factors for the force field, and setting suitable empirical criteria for different types of Fermi resonances (FR) and Darling–Dennison resonances (DD). There is extensive literature illustrating the difficulties with the various procedures listed.

Due to high biological importance as one of the four RNA nucleobases, uracil (Figure 1) has been extensively studied by various physical-chemical, nondestructive spectroscopic techniques for more than 50 years.[2−60] Because of its very low vapor pressure (75 mTorr at 210 °C),[7] vibrational spectra and other molecular properties of uracil were mostly studied in various condensed states. Data for isolated molecules are relatively rare.

The diketo tautomer of uracil (2,4(1*H*,3*H*)-pyrimidinedione) is estimated to be ca. 10 kcal mol^{-1} lower in energy than the keto–enol and dienol tautomers according to the QM model

Received: April 3, 2015
Revised: May 28, 2015
Published: May 28, 2015

DOI: 10.1021/acs.jpca.5b03241
J. Phys. Chem. A 2015, 119, 6723−6737

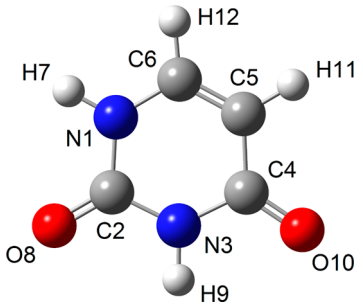

Figure 1. Structural formula and numbering of atoms of uracil.

MP2/6-311++G(d,p)[46] (see also ref 32) and has been observed as a single tautomer in the gas phase. A partial semiexperimental equilibrium structure (r_e^{se}) was derived by Puzzarini et al.[55] from previously determined microwave (MW) ground state rotational constants for 10 isotopologues[23,46] corrected for rotation−vibration effects with the use of the B3LYP/N07D cubic force field. This structure was reanalyzed by Császár et al.[60] with the application of the mixed regression method and with the use of the rovibrational corrections calculated from the B3LYP/6-311+G(3df,2pd) cubic force constants. The equilibrium structure of uracil was also determined by Vogt et al.[58] from the gas electron diffraction (GED) data corrected for harmonic and anharmonic vibrational effects with the use of the MP2(fc)/cc-pVTZ force field. It has been also shown[58,60] that the semiexperimental structures r_e^{se}(GED) and r_e^{se}(MW) agree well both with each other and with the best ab initio one. This theoretical structure, r_e(best), was computed at the level of the coupled cluster method with single and double excitations and a perturbative treatment of connected triples, CCSD(T)(fc)[55,60] or CCSD(T)(ae)[58] [fc and ae denote valence (frozen core) and all electron correlation]. The basis set was the correlation-consistent polarized weighted core valence triple-ζ basis set, cc-pwCVTZ, further extrapolated to the quadruple-ζ basis set, cc-pwCVQZ, at the level of the second-order Møller−Plesset perturbation theory, MP2(ae)[58] (see also refs 55 and 60 for an alternative extrapolation) with an inclusion of diffuse-function corrections (aug).

IR spectra of uracil have been measured in a solid state (polycrystalline) form[2−4,31,35] and in a gas phase (vapor).[5,37] IR spectra have also been observed for material trapped in a low-temperature matrix-isolated form,[10,11,16−18,25,26,28,30,33,39] cooled in a pulsed slit jet,[34] dispersed in jet-cooled helium nanodroplets,[47] and dissolved in solution.[13,35,42] RS spectra have been measured both in the solid state[3,35] and in polycrystalline form.[4,27,31,35] Resonance RS spectra were studied in solution,[20] as were normal RS spectra.[35] RS were also studied with matrix isolation.[16] A neutron inelastic scattering (NIS) spectrum of a polycrystalline sample of uracil was also obtained.[35,36]

Numerous studies were devoted to the calculation of normal modes of uracil using purely empirical or semiempirical QM harmonic force fields[4,8,12,31] and scaled *ab initio* harmonic force fields (SQMFF).[9,15,21,22,29−31,35,36,38−41,47,51,53,56] Bandekar and Zundel[14] undertook a normal coordinate analysis on a unit cell of uracil. The problem of interpretation of spectra in the light of multiple Fermi resonances was first discussed in ref 24 and subsequently in refs 33, 52, and 54. More recently, anharmonic calculations of fundamental and multiquanta transitions of uracil were performed in a number of papers.[44,45,48,52,54,55,59] The most advanced analysis of vibrational spectra was carried out by Puzzarini et al.[54] by comparison of experimental frequencies with the theoretical counterparts computed with the use of the best estimated CCSD(T)-based harmonic force field (see the section "The Method of Calculation" below for details) in combination with the B3LYP (in conjunction with the aug-N07D and aug-cc-pVTZ basis sets) anharmonic force constants (hybrid model).[54]

Although abundant literature on modeling and interpretation of spectral features of uracil exists, none of the recent anharmonic theoretical studies[44,45,48,52,54,59] simultaneously analyzed available experimental IR and RS data, employed high-level theoretical methods [MP2 and CCSD(T)], used predicted IR and RS intensities for spectral interpretations, theoretically analyzed FR splittings and vibrational polyads, and employed systematic criteria for vibrational resonances. As recently noted by Katsyuba et al.,[57] "there are still significant doubts on the interpretation of the IR spectrum of isolated uracil, the main problem being the large number of overtones and combination bands having intensities comparable to those of some fundamentals".

The most recent work by Fornaro et al.[59] is devoted to the study of a series of nucleobases and only a small discussion is devoted to uracil itself. Besides, both recent studies of essentially the same researchers' group[54,59] use only a limited number of references as a source of experimental data,[10,26] whereas the assignments vary among publications without a discussion. The most recent work[59] compared the performance of different density functional theory (DFT) approaches using as a criterion of success the mean absolute errors (MAE) between calculations and experiment. However, the experimental data for comparison were not always chosen from the best sources.

In the present study we employed our systematic implementation of the anharmonic vibrational canonical Van Vleck perturbation theory in an essentially analytic operator form,[61−67] as well as PES and MPS obtained by a purely *ab initio* method (MP2). This approach is enhanced by harmonic frequencies obtained at higher theoretical level. In addition, we used the most reliable sources of the experimental data accompanied by a detailed discussion of assignments. There are several important principles that we put forward and defend in our theoretical research that distinguish our work from competing approaches employed by other groups.

First, we use advanced theoretical models of molecular vibrations that directly describe experimentally observed phenomena, such as energy levels of anharmonic vibrational states, which can be measured with very high accuracy, as well as vibrational intensities in IR and RS spectra. For example, a commonly used *double-harmonic* approximation produces harmonic frequencies and intensities based on quadratic force fields and first derivatives of the electro-optical parameters (dipole moment and polarizability tensor components). The difference between observed frequencies and their harmonic counterparts can be so large (over 100 cm^{-1}) that such predictions can be of little use for interpreting spectra. Empirical corrections of the data, such as scaling of the harmonic force fields,[68,69] or direct scaling of harmonic frequencies[70−72] become unavoidable. Doing so introduces a substantial element of arbitrariness and requires a large amount of manual work and the application of expert knowledge.

Second, modeling of experimentally observed spectra also requires an accurate theoretical description of energies and

DOI: 10.1021/acs.jpca.5b03241
J. Phys. Chem. A 2015, 119, 6723−6737

intensities of nonfundamental transitions, such as overtones and combination bands that in some cases can be even more intense than fundamental bands. In addition, the frequencies of such bands are very sensitive to small structural variations and may represent a part of the so-called "fingerprint" of a molecule. It is well-known that the double-harmonic approximation is of little use for such bands. Another very important part of the nonfundamental vibrational phenomena is a Fermi resonance (and the higher-order resonance effects as well) and associated shifts of vibrational energy levels and redistribution of the intensities between "bright" and "dark" states. As it is very well-known from the literature, Fermi (as well as Darling–Dennison) resonances play a major role in certain regions of uracil spectra.[24,33,52,54]

An efficient theoretical approach, suited to most of the targets outlined above, is based on a solution of the vibrational Schrödinger equation using perturbation theory. Because the "zero-order" harmonic problem (Wilson GF-method[73]) is amenable to an analytic solution, it is very convenient to consider a solution of a vibrational problem with a harmonic potential amended by cubic and quartic anharmonic terms as a perturbation of the zero-order problem. Vibrational perturbation theory has been successfully developed since the early work of Nielsen and co-workers.[74−80] The outcome of this theory is a set of closed expressions for such quantities as anharmonic constants, zero-point vibrational energy (ZPVE), IR and RS activities of fundamental and nonfundamental transitions, and expressions for Fermi and Darling–Dennison resonance coupling constants.[74−107] We call it an analytic version of second-order perturbation theory (AVPT2). However, evaluation of precise values of spectroscopic characteristics requires an additional stage with an essentially numerical calculation, based on a matrix diagonalization.

Resonance phenomena introduce significant complications in the evaluation of the above quantities. A correct treatment of the problem requires building the reduced matrix representation of the Hamiltonian, comprising the most important resonance off-diagonal couplings. After a suitable set of zero-order basis functions is chosen and the corresponding matrix elements are calculated, the Hamiltonian must be numerically diagonalized to obtain the final perturbed anharmonic frequencies and eigenvectors containing information about the resonance mixing of vibrational states. The values of the off-diagonal Hamiltonian terms can also be evaluated in a form of closed expressions, derived using the vibrational perturbation theory in analytic form. Although the expressions for the first-order Fermi-resonance couplings (*W*-constants) are quite simple,[78] descriptions of the second-order couplings (*K*-constants), which can be collectively called "Darling–Dennison" resonances,[102−107,65] require more sophisticated expressions, whose correct form was finally derived only very recently by Rosnik and Polik.[107] This amended two-stage procedure can be collectively called by the abbreviation AVPT2+*WK*. Overall, a computer implementation of the AVPT2+*WK*, including the numerous cumbersome expressions for Darling–Dennison resonance constants and transition moments, is a nontrivial problem. It is very difficult to ensure that all formulas are correct and properly transformed into a computer code. There are the additional complications of choosing systematic criteria for different types of resonances and the systematic theoretical shortcoming of AVPT2+*WK* that manifests itself in the interference of Fermi and Darling–Dennison resonances and leads to the incorrect evaluation of the latter ones.[65] Second-order perturbation theory can be most efficiently implemented using a theoretical technique, called a numeric-analytic operator version of Canonical Van Vleck Perturbation theory (CVPT2+*WK*).[108−113]

The traditional implementation of VPT2 in the form of closed expressions for different quantities (such as anharmonic constants, resonance constants, ZPVE, transition strengths etc.), collectively called AVPT2+*WK*, is fast and can be applied to rather large molecules. An alternative implementation of VPT2 in the form of CVPT2+*WK* is more precise and thorough in the treatment of Darling–Dennison resonances and the evaluation of infrared and Raman intensities. In addition, for smaller molecules CVPT can be seamlessly extended to fourth order. Because both implementations (AVPT2+*WK* and CVPT2+*WK*) represent essentially the same theoretical approach (VPT2), parallel implementation of them is a convenient mean of debugging of computer code. The size of the uracil molecule (12 atoms and 30 degrees of vibrational freedom) permits application of our major CVPT2+*WK* method.

2. THEORY

The universal method of solving of the vibrational Schrödinger equation (AVPT2+*WK*), usually referred to as simply "VPT2", is based on a set of closed expressions for evaluation of the anharmonic constants (x) as well as Fermi (W) and Darling–Dennison (K) resonance constants.[65,74−93,102−107] Such expressions can be obtained using customary Raleigh–Schrödinger perturbation theory (RSPT).[77,106] As mentioned above, an alternative approach is based on an operator version of the canonical Van Vleck perturbation theory (CVPT), typically limited to the second order, and also requiring the variational stage (CVPT2+*WK*).[108−113,62] CVPT2+*WK* performs a series of canonical transformations for the explicit operator representation of the Hamiltonian, reducing to a quasi-diagonal form every time when the Schrödinger equation is solved. These operator transformations can be performed explicitly using the numerical-analytic technique.[62,112] We consider the differences between these methods in detail below.

As usual, for the perturbative solution of the vibrational Schrödinger equation, we begin with the second-order vibrational Watson-type Hamiltonian, expressed in powers of the dimensionless rectilinear normal coordinates $q_r = Q_r[4\pi^2c^2\omega_r(hc)^{-1}]^{1/2}$ (here ω_r and Q_r are harmonic frequencies and Wilson's normal coordinates, and c and h are universal constants), and the conjugate momenta $p_r = -\mathrm{i}(\partial/\partial q_r)$. Limiting our consideration to a nonlinear asymmetric top N-atomic molecule with $M = 3 \times N - 6$ vibrational degrees of freedom, we present Hamiltonian in the following familiar form:[78]

$$H = \left[\frac{1}{2}\sum_r \omega_r(p_r^2 + q_r^2)\right] + \left[\frac{1}{6}\sum_r\sum_s\sum_t \varphi_{rst}q_rq_sq_t\right] + \left[\frac{1}{24}\sum_r\sum_s\sum_t\sum_u \varphi_{rstu}q_rq_sq_tq_u + \sum_{\alpha=x,y,z} B_e^{\alpha}\left(\sum_r\sum_s\sum_t\sum_u \zeta_{rs}^{\alpha}\zeta_{tu}^{\alpha}\left(\frac{\omega_s}{\omega_r}\right)^{1/2}\left(\frac{\omega_u}{\omega_t}\right)^{1/2} q_rp_sq_tp_u\right)\right] \quad (2.1)$$

DOI: 10.1021/acs.jpca.5b03241
J. Phys. Chem. A 2015, 119, 6723−6737

Here, ϕ_{rst}, etc. are force constants, the B_e^α are equilibrium rotational constants (both in cm^{-1} units), and the ζ_{rs}^α are dimensionless Coriolis vibration−rotation coupling constants.

In the framework of CVPT2 methodology, the Hamiltonian equation (2.1) is subjected to a series of canonical transformations that do not change the spectrum of the operator but do alter its eigenfunctions.[74−80,108−113] The aim is to make the transformed eigenfunctions coinciding with the zero-order harmonic oscillator basis functions which makes the integration of the final form of the transformed Hamiltonian with the zero-order harmonic oscillator basis set a straightforward problem. The canonical transformations can be reduced to adding certain terms to the Hamiltonian arranged by the orders of perturbation theory, $H = H_0 + H_1 + H_2 = \Sigma H_K$. Such terms generally look like sums of nested commutators of parts H_K of the Hamiltonian with so-called S_K-operators that can be chosen in such a way that unwanted off-diagonal terms in the Hamiltonian are canceled after the summation.[74−80,108−113] After summation of the zero-, first-, and second-order terms of the twice canonically transformed Hamiltonian, one obtains a familiar expression:[78]

$$\hat{H}^{(2)} = H_0 + H_1 + \mathrm{i}[S_1,H_0] + H_2 + \mathrm{i}[S_1,H_1] - \frac{1}{2}[S_1,[S_1,H_0]] + \mathrm{i}[S_2,H_0] \tag{2.2}$$

It can be shown[110] that to obtain the desired form of the effective Hamiltonian as a function of vibrational quantum numbers $\bar{v} = \{v_1, v_2 ... v_M\}$, it is sufficient to evaluate the diagonal matrix elements of once canonically transformed Hamiltonian, which is given by[78]

$$\langle \Psi_A(\bar{v})|\hat{H}^{(1)}|\Psi_A(\bar{v})\rangle = \langle \Psi_A(\bar{v})|H_0 + H_2 + \frac{1}{2}\mathrm{i}[S_1,H_1]|\Psi_A(\bar{v})\rangle \tag{2.3}$$

The resulting expression is the familiar form of the Dunham-type energy expression, also called the effective Hamiltonian:[78]

$$E(\bar{v})(hc)^{-1} = E_0 + \sum_r^M \omega_r\left(v_r + \frac{1}{2}\right) + \sum_{r\le s}^M x_{rs}\left(v_r + \frac{1}{2}\right)\left(v_s + \frac{1}{2}\right) \tag{2.4}$$

An implementation of CVPT2+*WK* is certainly more computer intensive than working with AVPT2+*WK*, but CVPT2+*WK* has a number of advantages that outweigh the convenience of utilizing of analytic expressions derived once and forever. There are at least two major difficulties with AVPT2+*WK*. First, many cumbersome expressions are needed to cover all cases of Darling−Dennison resonance coupling coefficients and especially expressions for strengths of multiple types of transitions, including fundamental ones. Second, all these expressions must be cleaned of terms containing "resonance denominators" using certain resonance criteria. Doing so is not difficult for Fermi resonances but is much more complicated and insufficiently standardized for Darling−Dennison resonances.[65,104,107] In addition to the vibrational problem, thermodynamics requires a very accurate evaluation of the zero-point vibrational energy (ZPVE), and even the most recent publication on this subject contains an erroneous expression for ZPVE derived within AVPT2.[114]

An implementation of CVPT2+*WK* is rather a matter of programming effort with fewer principal expressions of a simple nature, and it is easy to maintain consistency in the intermediate and final results.[62] In addition, CVPT2+*WK* can seamlessly be extended to higher orders (fourth, sixth, etc.). Although such higher-order calculations require a steep increase in the computational cost of generating necessary higher-order terms in PES and MPS, it is worth the effort when such precision is necessary. Indeed, it was shown that the difference $\Delta\nu_r(2-4)$ in fundamentals calculated by CVPT2+*WK* and CVPT4+*WK* can be on the order of 3−4 cm^{-1}. In formaldehyde, for instance, $\Delta\nu_1(4-2)$ equals 3.4 cm^{-1}, and in 1,1-difluoroethylene, $\Delta\nu_1(4-2)$ equals 3.7 cm^{-1}. Regretfully, the costs involved for CVPT4+*WK* are prohibitive for molecules of the size of uracil.

Probably the major advantage of CVPT2+*WK* is that it ensures a more systematic and accurate treatment of resonances at any order. It was shown[65] that in certain situations that are typical for molecules bigger than simple 3−4 atomics, AVPT2+*WK* cannot generally produce correct values for Darling−Dennison constants (K). First- and second-order resonances interfere in such a way that a correct removal of resonance terms in general resonance-free expressions "post-factum" cannot be done. In addition, CVPT2 produces an explicit form of the S_K-operators so that any molecular property (such as a dipole moment vector or polarizability tensor components) that is expanded in a power series of normal coordinates can be also subjected to same canonical transformations for evaluation of the corresponding anharmonic properties.

A relative simplification in the implementation of CVPT2+*WK* is based on a transformation from the coordinate/momentum representation of the Hamiltonian eq 2.1 to an equivalent representation expressed in products of harmonic oscillator creation/annihilation operators $a^\dagger$, a (CAO):[109]

$$a^\dagger = \frac{1}{\sqrt{2}}(q - \mathrm{i}p) \qquad a = \frac{1}{\sqrt{2}}(q + \mathrm{i}p) \tag{2.5}$$

The original Hamiltonian must be converted to the CAO-representation using the following definitions:

$$q = \frac{1}{\sqrt{2}}(a^\dagger + a) \qquad p = \frac{1}{\sqrt{2}}\mathrm{i}(a^\dagger - a) \tag{2.6}$$

In addition, products of CAO should be reduced to a standard form using the normal ordering,[111,112]

$$H = \sum_j h_j \prod_{l=1}^M (a_l^\dagger)^{m_{jl}}(a_l)^{n_{jl}} \tag{2.7}$$

Here the summation on j is performed over all operator terms of the Hamiltonian with a scalar multiplier h_j and the integers m_{jl}, n_{jl} are powers of the corresponding CAO products. All subsequent transformed forms and parts of the Hamiltonian along with the S_K-operators and subsequently terms for the dipole moment and polarizability operators are kept in CAO representation preserving the normal ordering of elementary terms.

The S_K-operator that is needed for cancellation of the nonresonance off-diagonal terms after the final summations in eqs 2.3 or 2.4 can be obtained using the following expression,[109]

DOI: 10.1021/acs.jpca.5b03241
J. Phys. Chem. A 2015, 119, 6723−6737

$$S = -\mathrm{i}\sum_{j} h_j\Big(\sum_{l=1}^{M}(m_{jl}-n_{jl})\omega_l\Big)^{-1}\prod_{l=1}^{M}(a_l^{\dagger})^{m_{jl}}(a_l)^{n_{jl}} \tag{2.8}$$

Evaluation of the commutators $[S_K, H_L]$can be made through reduction to the standard form with normal ordering using the following equality:[112]

$$(a^{\dagger})^k a^l (a^{\dagger})^m (a)^n = (a^{\dagger})^{k+m}(a)^{l+n} + \sum_{i=1}^{\min(l,m)}\left[\left(\frac{1}{i!}\prod_{j=0}^{i-1}(l-j)(m-j)\right)(a^{\dagger})^{k+m-i}(a)^{l+n-i}\right] \tag{2.9}$$

with subsequent collection of like operator terms in the resulting operator polynomials. These polynomials can reach a very large size, but it is not necessary to keep them entirely in a computer memory and they can be conveniently stored in binary files and treated sequentially.

The most important remaining part of the CVPT2+*WK* calculation is a treatment of the resonance terms that can be recognized by "abnormally large" values of a dimensionless quantity Ω_k whereas the value of the denominator Δ_k does not exceed a certain limit $\Delta^{\dagger}$,[62−65]

$$\Omega_k = h_k\Big(\sum_{l=1}^{M}(m_{kl}-n_{kl})\omega_l\Big)^{-1} \qquad |\Omega_k| > \Omega^{\dagger}$$
$$\Delta_k = \Big(\sum_{l=1}^{M}(m_{kl}-n_{kl})\omega_l\Big)^{-1} < \Delta^{\dagger} \tag{2.10}$$

The crucial question is what terms can be called "abnormally large"? There are two ways to answer this difficult question because besides the simpler case of Fermi resonances[115,65] there are also various cases of Darling−Dennison resonances that can severely affect vibrational intensities.[93] First, the strategy can be based on an evaluation of quantities of Ω_k for well-studied cases, when repulsion of levels and redistribution of intensities is without doubt. Second, a systematic choice of resonance criteria is directly linked with the concept of vibrational polyad quantum numbers.[116−123,63−65] For a properly chosen set of resonance operators, the matrix of the canonically transformed quasi-diagonal Hamiltonian gains the block-diagonal structure. All basis functions for each block have an identical attribute: the polyad quantum number. The consequence is that resonance couplings are confined to blocks and no interblock couplings occur. It is convenient to analyze the connection between the manifold of resonances of a particular molecule and the structure of its vibrational polyads using the vector method introduced by Kellman.[116] In brief, the vector of integer coefficients defining the form of the polyad vector in the *M*-dimensional space of vibrational quantum numbers must be always orthogonal to vectors of integers representing vibrational resonances.[116,64] Armed with Kellman's method and analyzing the form of the polyad vector of a number of organic molecules of relatively small size, we have found that the dimension of the space spanned onto the manifold of resonance vectors, systematically selected by CVPT2+*WK*, typically equals the overall dimension of the space (the number of normal coordinates) less one.[64] This nontrivial result means that the form of the polyad vector is typically uniquely defined. The resonance picture becomes more blurred with an increase of the molecular size, and eventually polyad structure breaks down. However, the criteria for selecting resonances for well-defined cases of polyad structures of smaller molecules can be applied to larger molecules. We refer the reader for a more detailed description of the underlying theory in ref 64 and literature cited therein.

The final essential part of the theory needed for making the description of CVPT2+*WK* complete for the purpose of the vibrational analysis of uracil is evaluation of the IR and RS intensities. Typically, the point is that any scalar molecular property that is expanded in a Taylor series at the point of equilibrium in powers of dimensionless normal coordinates and arranged in the orders of smallness in the same way as it is done for the Hamiltonian itself can be canonically transformed using the S_K-operators obtained for the necessary reduction of the Hamiltonian. Because the resonance off-diagonal terms of the Hamiltonian are being canceled numerically at the final "-*WK*" stage, the eigenvectors of the numerical transformation hold the coefficients of mixing the molecular properties, partially transformed by the perturbation theory. This theory is well-established, and it can be applied to the evaluation of IR and RS intensities, once the molecular tensor properties such as dipole moment and polarizability are decomposed into scalar components and each component is treated independently.[93−101]

For example, if the α-component of the effective dipole moment operator $\mu_\alpha = \mu_\alpha(q)$, as a function of normal coordinates q_i, is expanded in a power series

$$\mu_\alpha(q) = \left[\mu_\alpha^{\,0} + \sum_r\left(\frac{\partial\mu_\alpha}{\partial q_r}\right)_0 q_r\right] + \left[\frac{1}{2}\sum_{rs}\left(\frac{\partial^2\mu_\alpha}{\partial q_r\partial q_s}\right)_0 q_r q_s\right] + \left[\frac{1}{6}\sum_{rst}\left(\frac{\partial^3\mu_\alpha}{\partial q_r\partial q_s\partial q_t}\right)_0 q_r q_s q_t\right] + \ldots \tag{2.11}$$

where the square brackets denote the zeroth, first, and second orders of VPT2, then, performing the double contact transformation, one obtains the effective dipole moment operator in the form:

$$\mathrm{M}_\alpha = \left(\mu_\alpha^{[0]} + \mathrm{i}[S_1,\mu_\alpha^{[0]}] - \frac{1}{2}[S_1,[S_1,\mu_\alpha^{[0]}]] + \mathrm{i}[S_2,\mu_\alpha^{[0]}]\right) + \left(\mu_\alpha^{[1]} + \mathrm{i}[S_1,\mu_\alpha^{[1]}]\right) + \mu_\alpha^{[2]} \tag{2.12}$$

The following formula can be applied for calculation of the integral absorption coefficient of the electric dipole moment $a \leftarrow b$ for the Boltzmann distribution of molecules at absolute temperature T:[79]

$$I^{(ab)} = \frac{8\pi^3 N_\mathrm{A}}{3hcQ}\nu^{(ab)}S^{(ab)}\left[\exp\left(-\frac{E^{(b)}}{kT}\right) - \exp\left(-\frac{E^{(a)}}{kT}\right)\right] \tag{2.13}$$

where N_A is the Avogadro number, k is the Boltzmann constant, $\nu^{(ab)}$ is the $a \leftarrow b$ transition wavenumber, and Q is the vibrational partition function. In eq 2.13 the line strength $S^{(ab)}$ of the dipole moment transition is given by[79]

$$S^{(ab)} = \sum_\alpha |\langle\Phi_0^{(a)}|\mathrm{M}_\alpha|\Phi_0^{(b)}\rangle|^2 \tag{2.14}$$

The effective dipole moment operator $\mu_\alpha = \mu_\alpha(q)$ can be easily converted into a CAO representation, and further evaluation of the transformed effective dipole moment operator in eq 2.14 and line strength in eq 2.13 can be accomplished.

DOI: 10.1021/acs.jpca.5b03241
J. Phys. Chem. A 2015, 119, 6723−6737

Tensor components of the polarizability operator $\alpha_{\xi\zeta}(q)$; $\xi, \zeta = x, y, z$ can be subjected to a series of canonical transformations in the same way as it is done above with components of the dipole moment.[95,125] The differential cross section $(\partial\sigma_j/\partial\Omega)$ of RS is typically used as a quantity characterizing the intensity of the jth ban:[124]

$$\frac{\partial\sigma_j}{\partial\Omega} = \frac{(2\pi)^4}{45}(\nu_0 - \nu_j)^4\left[1 - \exp\left(-\frac{hc}{kT}\nu_j\right)\right]^{-1}\frac{hc}{8\pi^2c^2\nu_j}S_{RS}(\nu_j) \tag{2.15}$$

Here ν_0 is the frequency of the excitation line, h, c, and k are universal constants, T is the absolute temperature, and Ω is the solid angle at which light is recorded. The quantity $S_{RS}(\nu_j)$ is called the coefficient of Raman scattering activity.[124]

The RS differential cross sections in the form of eq 2.15 includes the term $(\nu_0 - \nu_j)^4$, containing the frequency of the excitation line ν_0. This dependence can be removed by quoting the reduced quantity $S_{RS}(\nu_j)$, expressed in units of squared polarizability (Å^6), divided by units of squared normal coordinates Q^2 (Å^2 × amu), or by dimensionless squared normal coordinates q^2. As suggested in ref 124, the modified quantity $(\partial\sigma_j/\partial\Omega)(\nu_0 - \nu_j)^{-4}$, where the excitation line dependence is moved to the left side of eq 2.15 and therefore introducing the absolute normalized differential cross section of RS, expressed in units Å^6/sr = 10^{-48} cm^6/sr, which will further be abbreviated as RSU.

3. THE METHOD OF CALCULATION

We have chosen CVPT2+*WK* as the main method of our calculation of the anharmonic spectrum of uracil. The detailed methodology of CVPT2+*WK* has been previously described in several publications.[61−67] In this section, we describe a number of practical matters that are more specific for uracil because of its size and provide additional essential specifications.

All vibrational calculations were performed using an upgraded software package ANCO (acronym for analysis of normal coordinates).[61,62,64,65] The current version of ANCO has a wide functionality that includes various force field transformations, the traditional AVPT2+*WK* implementation for calculation of anharmonic vibrational spectra (including IR and RS intensities) for molecules containing up to 40 atoms, and an efficient utilization of the numerical-analytic CVPT2+*WK* calculations for molecules containing up to 12 atoms. The unique implementation of optimized numerical-analytic algorithms for conversion of the original Hamiltonian to CAO representation, storage, and manipulations with operator CAO polynomials of very large size (containing up to hundreds of millions of individual operator terms), such as evaluation of commutators (single and nested), collection of like terms, integration, etc., enables performance of a single CVPT2+*WK* calculation for uracil on a desktop computer in about 3 h. The efficiency of the calculations rests upon an algorithm of encoding-decoding of a single arbitrary Hamiltonian (eq 2.7) and *S*-operator (eq 2.8) term of the kind kept as "long" (eight byte) integers, so that a comparison of operators for the most computationally intense stage of collection of like terms becomes an elementary operation of comparing two integers.

The Gaussian'09 program package (G09)[126] has been utilized for the geometry optimizations and evaluations of PES and MPS only and has been integrated with the ANCO package through the Gaussian input-output (including ASCII checkpoint) file-based interface. The Cartesian harmonic force constants (Hessian matrix), as well as values and first derivatives of the dipole moment and polarizability of uracil, were calculated by G09 at the point of equilibrium and at displaced configurations.

The optimized geometry of uracil in the form of G09 Z-matrix, the independent set of internal coordinates and the harmonic force field in both Cartesian and internal coordinates can be found in the Supporting Information. The numbering of atoms of uracil is presented in Figure 1.

In the first stage, the MP2 method along with the Dunning correlation-consistent triple-ζ basis set (cc-pVTZ) has been employed for calculation of the harmonic force field and normal coordinates. Afterward, normal mode finite displacements in Cartesian coordinates were generated for calculation of the "semi-diagonal" quartic potential energy surface by a single-dimension numerical differentiation of Hessians (analytical second derivatives of the electronic energy in Cartesian coordinates), using the 9-point equidistant grid, and a 0.02 Å × (amu)$^{1/2}$ step size. Calculation of the cubic surfaces of the dipole moment and the quadratic surfaces of the polarizability tensor components were performed by the single and double differentiation of the analytic dipole moment first derivatives and the polarizability, respectively.

It was realized by a number of researchers some time ago that the major source of inaccuracy in anharmonic vibrational calculations is in inadequate harmonic frequencies. An efficient and economical solution of the problem is a combination of the highest accuracy of advanced QM models [such as CCSD(T)] for evaluation of the harmonic part of the PES only, and application of economical models (such as DFT or MP2) for calculation of higher derivatives. This concept has been widely used in various studies and is called a "hybrid" force field.[127,128] In our study of uracil we have utilized the hybrid PES by the replacement of the MP2/cc-pVTZ harmonic frequencies by the "best theoretical" values computed in ref 54 as follows:

$$\omega(\text{best}) = \omega(\text{CBS}) + \Delta\omega(\text{CV}) + \Delta\omega(\text{aug}) + \Delta\omega(\text{T}) \tag{3.1}$$

Here $\omega(\text{CBS}) = \omega(\text{MP2(fc)/cc-pVQZ}) - \omega(\text{MP2(fc)/cc-pVTZ})$ is an extrapolation to the complete basis set (CBS) limit; $\omega(\text{CV}) = \omega(\text{MP2(ae)/cc-pCVTZ}) - \omega(\text{MP2(fc)/cc-pCVTZ})$ is a correction due to core−valence (CV) correlation; $\omega(\text{aug}) = \omega(\text{MP2(fc)/aug-cc-pVTZ}) - \omega(\text{MP2(fc)/cc-pVTZ})$ is a correction for diffuse function effects. Higher-order electron-correlation energy contributions ($\Delta\omega$(T)) have been derived by comparing the harmonic frequencies at the MP2/cc-pVTZ and CCSD(T)/cc-pVTZ levels.[54]

An essential part of the CVPT2+*WK* calculations is a systematic choice of the resonance criteria for both Fermi and Darling−Dennison resonances (eq 2.10). According to our experience, a suitable threshold value of the "resonance index" $\Omega^\ddagger$ is 0.05 (dimensionless), and a suitable threshold value of a "resonance denominator" $\Delta^\dagger$ is 300 cm^{-1}. Small variations of these empirical thresholds is not critical for the results. These resonance criteria can be adapted for use within the standard AVPT2+*WK* approach. We refer the reader to ref 65 for more details.

For a computationally convenient and accurate accounting of contributions of all Fermi and Darling−Dennison resonance operators to the Hamiltonian matrix elements related to pairs of basis functions, it is convenient to assemble all types of resonance operators together in a polynomial $\hat{R}$. Then, any

DOI: 10.1021/acs.jpca.5b03241
J. Phys. Chem. A 2015, 119, 6723−6737

Table 1. Harmonic (MP2/cc-pVTZ), "Best Theoretical" Harmonic,[b] Fundamental Anharmonic Frequencies, and IR/RS Intensities of Uracil Calculated by CVPT2 Using the Hybrid MP2/cc-pVTZ//"Best Theoretical"[b] Semidiagonal Quartic Force Field[a]

mode	harm., MP2	harm., "best"[b]	anharm, CVPT2	IR intensity	RS intensity	obsd IR and RS (where indicated) frequencies in gas and argon matrices[c]	description of FR and polyads (POL)[d]
1	3669.4	3652.7	3486.3	105	15.2	**3484** (s) gas;[e] 3484.3;[f] 3493.9 (He nanodroplets)[g]	resonance free
2	3616.4	3602.2	3435.2	63.5	11.3	**3436** (s) gas;[e] 3434.5 (48);[f] 3443.9 (He nanodroplets)[g]	resonance free
3	3292.0	3252.8	3133.6	1.30	5.7	**3124** (m) gas;[e] 3130 Ar[h]	FR: ν_3 (40%) & $\nu_6+\nu_{10}$
4	3246.5	3217.5	3081.0	0.58	6.7	**3084** (m) RS(Ar)[i]	FR: ν_4 (43%) & $\nu_7+\nu_8$
5	1828.6	1790.0	1761.2	364	1.9	**1764** (vs), 1762 (m) RS(Ar)[i]	POL: ν_5 (41%) & $\nu_{12}+\nu_{18}$ & $\nu_{10}+\nu_{21}$
6	1790.4	1761.5	1729.5	131	8.1	**1728** (vs), 1733 (m) RS(Ar)[i]	POL: ν_6 (29%) & $\nu_{12}+\nu_{20}$ & $\nu_{15}+\nu_{17}$
7	1686.2	1677.5	1642.8	27.6	5.6	**1641** (s);[e] 1644 (17);[f] 1643 (m), 1647 (s) RS(Ar)[i]	resonance free (93%)
8	1513.4	1505.4	1462.7	81.1	2.6	**1461** (s) gas[e]. 1472 (ms)[i]	FR: ν_8 (64%) & $\nu_{16}+\nu_{18}$ & $\nu_{14}+\nu_{21}$
9	1427.2	1427.2	1394.1	36.9	0.42	**1400** (s) gas;[e] 1399 (vs)[i]	resonance free (80%)
10	1413.3	1414.0	1382.0	69.1	2.8	**1387** (s) gas;[e] 1389 (m)[i]	resonance free (83%)
11	1389.2	1394.0	1351.0	7.66	3.6	**1356** (sh, m) gas;[e] 1359.3 (1.5);[f] 1360 (vw), 1360 (m) RS(Ar)[i]	FR: ν_{11} (53%) & $\nu_{25}+\nu_{26}$
12	1246.8	1248.2	1214.4	2.00	10.1	**1217** (w), 1220 (s) RS(Ar);[i] 1217.4 (1)[f]	resonance free (88%)
13	1212.3	1205.3	1179.9	98.8	0.37	**1187** (s) gas;[e] 1183 (0.24)[j]	resonance free (90%)
14	1095.3	1084.2	1060.8	6.67	1.4	**1066** (w), 1073 (w);[i] 1068.7 (3), 1075.5 (3)[f]	FR: ν_{14} (76%) and $2\nu_{19}$
15	992.7	995.4	979.9	4.59	0.15	**984.7** IR(Ne), 987.5 (0.8), 981.5 (0.7);[f] 990, 972 (sh, m) gas[e]	FR: ν_{15} (84%) & $\nu_{27}+\nu_{28}$
16	977.0	967.7	947.5	10.4	2.1	**952** (w) gas;[e] 958.3 (4);[f] 958 (w) IR,RS(Ar);[i] 958[h]	resonance free (83%); interferes with ν_{22}
17	774.9	772.8	751.8	1.29	10.9	**761** (s) RS(Ar);[i] 759.2 (1)[f]	FR: ν_{17} (69%) and $2\nu_{28}$
18	559.0	545.3	535.3	0.04	0.68	**538**;[k] 536 (w);[i] 536.4 (4)[f]	FR: ν_{18} (47%) & ν_{19} (45%)
19	538.1	540.8	531.1	7.44	6.3	**528**;[k] 516.5 (12)[f]	FR: ν_{19} (48%) & ν_{18} (24%) & $\nu_{28}+\nu_{29}$
20	515.4	517.2	510.8	16.1	2.4	**512** (w) gas[e]	resonance free
21	385.7	387.4	385.6	19.1	3.0	**395** (w) gas[e]	resonance free
A″							
22	968.9	973.3	955.9	0.45	1.2	**958** (w) RS (Ar)[i]	resonance free; interferes with ν_{16}
23	817.8	813.6	803.2	51.6	0	**802** (w) gas;[e] 804.0 (22)[f]	resonance free
24	762.8	765.2	756.1	29.2	0	**757** (w) gas;[e] 756.5 (12)[f]	resonance free
25	735.2	727.6	715.8	8.92	1.6	**717** (w) gas;[e] 717.4 (3)[f]	resonance free
26	691.6	670.3	651.4	32.4	0.50	**660** (w) gas;[e] 661.5, 657.9 IR(Kr);[f] 661 (0.17), 657 (0.05) IR(Ar)[j]	FR: ν_{26} (48%) & $\nu_{20}+\nu_{30}$
27	562.2	558.7	549.4	42.4	0.10	**545** (w) gas;[e] 551.2 (24)[f]	resonance free
28	394.8	387.9	384.4	24.0	0.65	**374** (vw) gas[e]	resonance free
29	163.2	159.1	157.9	0.30	3.9	**166**[k,l]	resonance free
30	146.4	140.4	139.7	0.82	0.04	**149** UV[m]	resonance free

[a]IR intensities are presented in units of km/mol; RS absolute normalized cross sections are presented in units of 10^{-48} cm^6/sr. [b]According to eq 3.1 (see text). See also ref 54. [c]Relative intensities are given in parentheses. Bold figures indicate chosen reference experimental values of fundamentals. [d]Resonance free: the share is not indicated when it is >95%. [e]Reference 37. [f]Reference 33. [g]Reference 47. [h]Reference 10. [i]Reference 16. [j]Reference 11. [k]Reference 35. [l]Reference 36. [m]Reference 19.

matrix element can be evaluated directly by using the following expression:

$$H_{ij} = \langle \Psi_0^{(i)}(\overline{\nu}_i) | \sum_l \hat{R}_l | \Psi_0^{(j)}(\overline{\nu}_j) \rangle \tag{3.2}$$

where an individual resonance operator is given by

$$\hat{R}_l = R_l \prod_{k=1}^{M} (a_k^{\dagger})^{m_{lk}} (a_k)^{n_{lk}} \tag{3.3}$$

Within our CVPT2+*WK* implementation, the operator polynomial $\hat{R}$ is generated automatically.

For the comprehensive consideration of the CVPT2+*WK* procedure, it is necessary to understand how to choose optimally the basis sets for the matrix representation of the Hamiltonian at the variational "+*WK*" stage. In the framework of an automated procedure, one can include all states $\Psi_0(\overline{\nu})$ with total vibrational excitation limited to N_{max}, which is defined as follows:

$$\Psi_0(\overline{\nu}) = \prod_{k=1}^{M} \psi_k^{(0)}(\nu_k) \qquad \sum_{k=1}^{M} \nu_k \le \mathrm{N}_{max} \tag{3.4}$$

The quantum number for every degree of freedom can be chosen equal to two, three, or four, for example. In the case of the uracil molecule, the setting of N_{max} = 4 would lead to an excessively large basis set, whereas the values of N_{max} = 2 and 3 correspond to more realistic values of 495 and 5455 basis functions, respectively. Our experience shows that increasing the size of the basis set in the case of a rather large molecule,

DOI: 10.1021/acs.jpca.5b03241
J. Phys. Chem. A 2015, 119, 6723−6737

such as uracil, can be counterproductive. Formally, increasing the size of the vibrational basis set leads to more accurate results. On the contrary, adding more basis functions causes redistribution of intensities among extra number of "dark" states. As a result, it can become more difficult to identify essential states corresponding to observed vibrational transitions. General spectroscopic experience shows that sufficiently weak resonances (with the share of dark states less that 5−10%) do not produce additional observable peaks. Therefore, in a majority of situations (although this is not a general rule) adding irrelevant triply excited states (or more) can spoil the picture by prediction of additional intense states that do not help in making vibrational assignments of observed peaks. Therefore, for our final calculation and spectral simulations we limited the basis set by allowing only single and double excitations (N_{max} = 2). With this setting, the CPU time on a desktop computer for a single CVPT2+*WK* calculation was about 3 h.

In the case of significant mixing of states, the quantitative description of a state can be given by percentages of the main zero-order basis functions participating in perturbed anharmonic states. The corresponding shares are trivially evaluated as squared components of eigenvectors obtained after the diagonalization of the Hamiltonian matrix, multiplied by 100%.

For elucidation of the vibrational assignments for the most problematic part of uracil spectra with multiple resonances (1790−1680 cm^{-1}), we employed spectral simulations to build a graph showing the overall curve produced by a superposition of peaks, taking their positions E_j and IR intensities $I_j^{(IR)}$ (in km/mol) as input data. To model spectra a standard Lorentzian function,

$$L_j(x) = I_j^{(IR)} w\pi^{-1}[(E_j - x)^2 + w^2] \quad (3.5)$$

with a half-width w = 1 cm^{-1} and a grid step of 0.1 cm^{-1} was utilized.

4. RESULTS AND DISCUSSION

In our vibrational analysis, we are relying on and quoting a selected set of the most accurate experimental studies of vibrational IR and RS spectra, because a comprehensive analysis of all existing spectral studies on uracil is beyond the limitations of this publication. The studies on uracil vibrational spectra that we used as the main sources of experimental data include the following: Colarusso et al.,[37] IR spectra in the gas phase; Aamouche et al.,[35,36] NIS, IR, and RS spectra in polycrystalline state and aqueous solutions; Ivanov et al.,[33] Les et al.,[30] Graindourze et al.,[26] Maltese et al.,[17] and Szczesniak et al.,[10] IR spectra of uracil trapped in nitrogen, argon, krypton and neon matrices; and Barnes et al.,[16] IR and RS spectra in argon and nitrogen matrices.

In our work, we are mainly focused on assignments of fundamental transitions to observed vibrational bands. In cases of Fermi resonance dyads or polyads, we also attempted to find experimental counterparts of all "bright" states. In some cases we tried to assign nonfundamental transitions that have sufficient intensity to be observable, even without intensity gains from fundamental states. Our interpretation of the term "assignment" focuses on vibrational quantum numbers rather than on linking vibrational modes to deformations of chemical moieties. Although the latter interpretation of a vibrational assignment is widely used for chemical purposes, the former definition is more strict and universal regardless of the size of a molecule. A good description of the normal modes of uracil can be found, for example, in ref 41.

In subsections 4.1 and 4.2 below we consider the assignments of fundamental and a few nonfundamental transitions. The results of the vibrational assignments are summarized in Table 1.

4.1. Symmetry Block A′. Two fundamentals are responsible for N−H bond stretches and have frequencies above 3400 cm^{-1}. Colarusso et al.[37] measured these bands in the gas phase, ν_1 = 3484 cm^{-1} (s) and ν_2 = 3436 cm^{-1} (s). Choi and Miller[47] recently measured both frequencies and intensities of ν_1 and ν_2 in helium nanodroplets, obtaining values 3493.9 cm^{-1} (A = 117 km/mol) and 3443.9 cm^{-1} (A = 72 km/mol), respectively. Our calculation predicts the positions of these resonance-free bands and intensities at 3486.3 cm^{-1} (A = 105 km/mol) and 3435.2 cm^{-1} (A = 64 km/mol). Comparing the predicted frequencies with the gas-phase counterparts and the predicted intensities with the study of Choi and Miller,[47] we see that the uncertainties of our theoretical method for these fundamentals are on the order of ∼0.1% for frequencies and on the order of 10−15% for intensities, whereas the relative ratio of intensities is reproduced within 3%.

The C−H stretching fundamentals ν_3 and ν_4 participate in strong multiple Fermi resonances with the overtones $\nu_7+\nu_8$ and $\nu_6+\nu_{10}$ to form four bright states. The highest energy state (40% share of ν_3) with the theoretical value of 3133.6 cm^{-1} is observable both in the gas-phase IR spectrum,[37] 3124 cm^{-1} (m), and in an argon matrix,[26] 3130 cm^{-1}. The lowest energy state with the 43% share of ν_4 has a very small IR intensity but was observed in an RS spectrum at 3084 cm^{-1} (m),[16] although this peak was assigned to ν_3. Two remaining states with notable RS intensities and predicted frequencies of 3101 and 3111 cm^{-1} were not observed experimentally.

The region of ∼1650−1800 cm^{-1}, containing the A′ fundamentals ν_5 and ν_6 is probably the most complicated one for the vibrational analysis as it contains a multitude of strong IR bands[10,15,16,30,33,37] due to multiple resonances and intensity borrowing by "dark" states. An adequate theoretical description of this phenomenon requires a construction of an isolated block of the Hamiltonian matrix with inclusion of major relevant interacting states. After evaluation of necessary coupling coefficients, the block is diagonalized, producing perturbed eigenvalues and eigenvectors that define the intensity redistribution. Within our automated procedure, all one- and two-quanta zero-order states are included. An energy range of interest is selected, and states with significant IR and/or Raman intensities are subjected to manual study. As seen from the calculation, the fundamental states ν_5, and ν_6 are mixed with the following 12 combination states: $\nu_9+\nu_{21}$, $\nu_{10}+\nu_{21}$, $\nu_{11}+\nu_{21}$, $\nu_{12}+\nu_{18}$, $\nu_{12}+\nu_{19}$, $\nu_{12}+\nu_{20}$, $\nu_{13}+\nu_{18}$, $\nu_{13}+\nu_{19}$, $\nu_{13}+\nu_{20}$, $\nu_{15}+\nu_{17}$, $\nu_{16}+\nu_{17}$, and $\nu_{22}+\nu_{23}$.

For the fundamental ν_5, the calculation predicts the state 1761.2 cm^{-1} with IR intensity 364 km/mol and RS intensity 2 RSU. The share of ν_5 in the state is 41%, and it is mixed predominantly with $\nu_{12}+\nu_{18}$ and $\nu_{10}+\nu_{21}$. The corresponding observed[16] bands in an argon matrix are located in IR spectrum at 1764 cm^{-1} (vs) and in RS spectrum at 1762 cm^{-1} (m), correctly assigned to ν_5 by the authors of the experimental study.[16] The level of redistribution of the fundamental state ν_6 between dark states is more extensive. It occurs with similar shares in two states, 1729.5 cm^{-1} (29%, 131 km/mol, 8 RSU) and in 1753.4 cm^{-1} (27%, 77 km/mol, 10 RSU). Their observed counterparts are 1728 (vs) and 1761 cm^{-1} (vs) in the

DOI: 10.1021/acs.jpca.5b03241
J. Phys. Chem. A 2015, 119, 6723−6737

Table 2. Vibrational Polyad for the Region 1680−1800 cm^{-1}, Containing Fundamentals ν_5 and ν_6[a]

state no.	anharm frequencies[b]	IR intensity	RS intensity	obsd matrix IR and Raman (where indicated) frequencies	polyad description
1	1688.2	15.1	0.16	1698 (ms) (Ar) $\nu_{13}+\nu_{20}$;[c] 1698.4 (Ar), 1695.2 (Ne)[d]	$\nu_{13}+\nu_{20}$ (89%) & $\nu_{12}+\nu_{20}$
2	1697.0	119	4.32	1706 (vs) (Ar), RS: 1707 (m);[c] 1698.4 (Ar), 1695.2 (Ne)[d]	$\nu_{16}+\nu_{17}$ (66%) & ν_6 (16%)
3	1710.5	29.4	2.71	1706 (vs) (Ar), RS: 1707 (m);[c] 1706.4, 1705.3, 1703.5 (Ar), 1705 (Ne)[d]	$\nu_{13}+\nu_{19}$ (56%) & $\nu_{16}+\nu_{17}$ & ν_6 (8%)
4	1717.7	18.6	0.67	1718 (m) (Ar);[c] 1717.3 (Ar), 1716.1 (Ne)[d]	$\nu_{13}+\nu_{18}$ (78%) & $\nu_{12}+\nu_{20}$
5	1720.6	24.0	3.01	1718 (m) (Ar), RS: 1722 (m);[c] 1717.3 (Ar), 1716.1 (Ne)[d]	$\nu_{12}+\nu_{20}$ (60%) & $\nu_{13}+\nu_{19}$
6	1729.5	131	8.11	**1728** (vs) (Ar), RS: 1733 (m);[c] 1728;[e] 1728.2, 1731.3, 1730.3 (Ar), 1732.3 (Ne)[d]	ν_6 (29%) & $\nu_{12}+\nu_{20}$ & $\nu_{15}+\nu_{17}$ & $\nu_{13}+\nu_{19}$
7	1735.7	65.1	0.84	1733 (s), 1731 (s) (Ar);[c] 1733.2 (Ar), 1738.1 (Ne)[d]	$\nu_{15}+\nu_{17}$ (68%)
8	1741.8	13.8	0.89	1741 (s) (Ar);[c] 1741 (Ar), 1740.8, 1744.4 (Ne)[d]	$\nu_{11}+\nu_{21}$ (85%)
9	1752.2	52.5	0.22	1757 (vs) (Ar);[c] 1757.5 (Ar), 1757.8 (Ne)[d]	$\nu_{12}+\nu_{18}$ (64%) & $\nu_{22}+\nu_{23}$
10	1753.4	77.6	9.82	1761 (vs) (Ar), RS: 1762 (m) (Ar);[c] 1760;[e] 1761.4 (Ar), 1757.8 (Ne)[d]	ν_6 (27%) & $\nu_{12}+\nu_{19}$ (36%) & ν_5 (13%)
11	1758.3	10.5	0.28	1762.8 (Ar), 1757.8 (Ne);[d] 1762[e]	$\nu_{22}+\nu_{23}$ (75%) & $\nu_{12}+\nu_{19}$
12	1761.2	364	1.90	**1764** (vs) (Ar);[c] 1763.7 (Ar), 1766.7 (Ne)[d]	ν_5 (41%) & $\nu_{12}+\nu_{18}$ & $\nu_{10}+\nu_{21}$
13	1767.2	112	1.06	1774 (s) (Ar);[c] 1770.2 (Ar), 1772.2 (Ne)[d]	$\nu_{10}+\nu_{21}$ (79%) & ν_5 (18%)
14	1776.1	20.2	0.22	1774 (s) (Ar);[c] 1774.3 (Ar), 1776.1, 1779.3 (Ne)[d]	$\nu_9+\nu_{21}$ (94%)

[a]IR intensities are presented in units of km/mol, RS absolute normalized cross sections are presented in units of 10^{-48} cm^6/sr. Bold values indicate chosen fundamental bands. [b]Calculated using CVPT2 and hybrid MP2/cc-pVTZ//"best theoretical" (see eq 3.1 and ref 54) semidiagonal quartic force field. [c]Reference 16. [d]Reference 33. [e]Reference 11.

IR, and 1733 (m) and 1762 cm^{-1} (m) in RS spectra.[16] Because the harmonic frequencies for ω_5 and ω_6 differ by 28.5 cm^{-1}, and the band 1729.5 cm^{-1} is twice as intense as the band at 1753.4 cm^{-1}, we choose the former one as the main state for ν_6. This choice agrees with the assignment of Fornaro et al.[59] and corrects the assignment made in ref 56. Table 2 provides an assignment of other strong bands in the region, corresponding to the combination states enlisted above.

For convenience, the results displayed in Table 2 are visualized in Figure 2 in the form of a simulated IR spectrum,

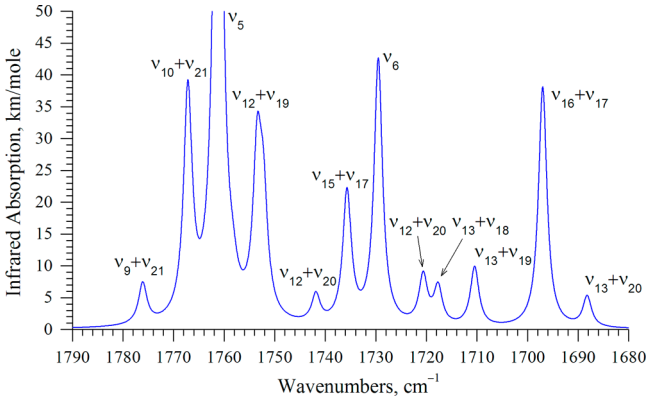

Figure 2. Simulated infrared spectrum of uracil in the region 1790−1680 cm^{-1}.

taking band positions and intensities as input data and modeling peaks with a Lorentzian function as explained above in section 3. Comparison of the simulated spectrum with the experimental ones from refs 33 and 39 shows a reasonable level of agreement between them.

It should be noted that in the case of multiple resonances and close-lying bright and dark states the resulting spectral picture can be very sensitive to small variations of zero-order vibrational frequencies. This is why a very accurate evaluation of harmonic frequencies is important to the accurate modeling of anharmonic spectra. The commonly found very complex nonlinear picture of resonance couplings and shifts of states makes some primitive models unreliable for reproducing the spectra by merely adjusting harmonic force fields or scaling of frequencies for a reliable interpretation of experimental spectra.

The assignment of ν_7 is much easier because this state is predominantly (93%) composed of the zero-order state. The calculated frequency 1642.9 cm^{-1} agrees well with the observed band in the IR spectrum at 1643 cm^{-1} (m) and in the RS spectrum at 1647 cm^{-1} (s).[16] In this spectral region there is one more intense IR band in an argon matrix at 1517 cm^{-1} (A = 6 rel. units).[33] Our calculation explains it as the overtone $2\nu_{17}$ with frequency 1518.4 cm^{-1} and IR intensity 4 km/mol that is evidently gained from nearby bright states.

The next fundamental ν_8 can also be easily assigned because the energy level 1462.7 cm^{-1} has the major share of the zero-order state (64%) and the major part of the IR intensity, 81.1 km/mol. Participation of other states is less than 10%. The corresponding bands observed in the gas-phase and argon-matrix IR spectra at 1461 cm^{-1} (s)[37] and 1472 cm^{-1} (ms),[16] respectively, were assigned to ν_8.[16]

The fundamentals ν_9, ν_{10}, and ν_{13} can be reliably assigned because they are very intense in the IR region and weakly interacting with dark states (share >80% of the zero-order state). The corresponding predicted frequencies of 1394.1 cm^{-1} (37 km/mol), 1382.0 cm^{-1} (69 km/mol), and 1180.0 cm^{-1} (99 km/mol) agree well with the observed IR gas-phase bands[37] of 1400 (s), 1387 (s), and 1187 (s) cm^{-1}. In this frequency region, there is an additional IR band at 1304 cm^{-1} (w)[16] that can be attributed to the overtone $2\nu_{26}$, because the theory predicts a peak 1290 cm^{-1} with IR intensity of 14 km/mol.

The resonance-free fundamental ν_{12} (1214.4 cm^{-1}) is quite weak in the IR spectrum but rather strong in the Raman spectrum (2 km/mol, 10 RSU). This band was not observed in the gas-phase IR spectrum,[37] whereas argon-matrix values[16] were measured at 1217 cm^{-1} (w, IR) and 1220 cm^{-1} (s, RS), respectively, and reproduce the theoretical approximate ratio between intensities. It should be noted that in matrix spectra site effects often produce bands that are close together, thus

DOI: 10.1021/acs.jpca.5b03241
J. Phys. Chem. A 2015, 119, 6723−6737

making the use of close bands for different fundamentals questionable.

The fundamental ν_{11} forms a strong Fermi resonance doublet with a combination state $\nu_{25}+\nu_{26}$ of 1351.0 cm^{-1} (53%, 7.7 km/mol, 3.6 RSU) and 1373.7 cm^{-1} (26%, 0.36 km/mol, 2.2 RSU). Both bands were observed experimentally in the gas phase,[37] 1356 cm^{-1} (sh,m) and 1371 cm^{-1} (sh,m) and in argon-matrix spectra,[16] 1360 and 1373 cm^{-1}, whereas slightly different values were obtained in another study at 1357 and 1378 cm^{-1}.[11]

A weak Fermi resonance with the overtone $2\nu_{19}$ takes place for the fundamental ν_{14}, forming a predicted doublet 1060.8 cm^{-1} (76% ν_{14} and 11% $2\nu_{19}$) and 1068.0 cm^{-1} (10% ν_{14} and 81% $2\nu_{19}$). The doublet is not resolved in the gas phase and is observed as a single band at 1082 cm^{-1} (m),[37] but in an argon-matrix-isolated form it is observed as a pair of bands at 1066 cm^{-1} (w) and 1073 cm^{-1} (w) with equal intensities.[16] In a neon matrix[33] two equally intense bands were also observed at 1072.3 and 1064 cm^{-1}. Our prediction correctly reproduces the FR separation of 7 cm^{-1} between the members of the dyad. The band with the lower frequency of 1066 cm^{-1} should be accepted as the ν_{14} fundamental, according to the predicted contributions of the zero-order states. Our choice differs slightly from the value of 1076 cm^{-1} for ν_{14} designated by Fornaro et al.[59] In this frequency region, there is one rather strong band in an argon matrix at 1100 cm^{-1} (w)[16] or 1102.4 cm^{-1} (A = 5 relative units).[33] Our calculation explains this band as an overtone $2\nu_{27}$ (1098.3 cm^{-1}) with unusually high IR intensity shared with a nearby state $\nu_{25}+\nu_{28}$. Barnes et al.[16] mistakenly explained this band as $2\nu_{18}$, which has a very low predicted intensity of 0.1 km/mol.

The fundamental ν_{15} with the predicted value of 979.9 cm^{-1} is rather weakly perturbed by a Fermi resonance with the combination band $\nu_{27}+\nu_{28}$ that lies considerably lower (~935 cm^{-1}). Its IR intensity is 4.59 km/mol, whereas the RS activity is quite small. According to Ivanov et al.,[33] in this region there are two peaks in an argon-matrix spectrum at 987.5 and 981.5 cm^{-1}, whereas in a neon-matrix spectrum only one peak was observed at 984.7 cm^{-1}. Barnes et al.[16] also observed only one weak peak in an argon matrix at 982 cm^{-1} (w), and the value was uncertain. Our theoretical calculation with the restriction of the maximum vibrational excitation to two quanta does not explain the reason for the appearance of the doublet. It can be due to participation of dark states with more quanta of excitation or a matrix site effect. We choose the neon-matrix value of Ivanov et al.;[33] it lies close to the argon-matrix value of Barnes et al.[16]

The fundamental ν_{16} is not perturbed by a Fermi resonance and is easily assignable. The predicted value of 947.5 cm^{-1} is in a good correspondence with both the gas-phase value of 952 cm^{-1} (w)[37] and the argon-matrix value of 958 cm^{-1} (w), in both IR and RS spectra.[16]

The fundamental ν_{17} is considerably perturbed by a Fermi resonance with a combination state $2\nu_{28}$. The state with the main share of the fundamental ν_{17} (751.8 cm^{-1}) is much stronger in the RS spectrum than in the IR spectrum, its Raman activity is 11 RSU vs 1.3 km/mol in the IR spectrum. The ν_{17} state is very close to the predicted frequency of an A″ fundamental ν_{24} (756.1 cm^{-1}), which has a very strong IR intensity (A = 29 km/mol), thereby making the IR observation of ν_{17} very difficult. However, the RS intensity of ν_{24} is nil, so that the argon-matrix RS band 761 cm^{-1} (s)[16] undoubtedly corresponds to ν_{17}. In the recent high-level theoretical anharmonic studies of uracil by Puzzarini et al.[54] and Fornaro et al.,[59] the quoted experimental value of ν_{17} was taken from IR matrix-isolation studies in refs 10 and 26, and the RS data were not considered. Because the bands for ν_{17} and ν_{24} lie very close to each other for the matrix-isolated form (757 and 759 cm^{-1}, lit.[26]) and are observed as a single peak 757 cm^{-1} (w) in the gas phase,[37] for a more reliable assignment it is essential to compare intensities in both the IR and Raman spectra. The Fermi resonance partner of ν_{17} is the combination state $2\nu_{28}$. The corresponding perturbed level at 777.8 cm^{-1} (69% of $2\nu_{28}$ and 30% of ν_{17}) has a predicted IR intensity of 3.39 km/mol and was observed experimentally by Susi and Ard[4] at 781 cm^{-1} (w) and erroneously assigned to ν_{17}.

The region 530−560 cm^{-1} is very complicated for assignments. It contains the states ν_{18} and ν_{19}, which are involved in multiple FRs, as well as ν_{27} (A″) near 549.4 cm^{-1}, which is very strong (predicted intensity 42 km/mol) in the IR spectrum and is a resonance-free state. The only IR gas-phase peak in this range at 545 cm^{-1} (w)[37] must correspond to ν_{27}. The IR argon-matrix-isolation study by Ivanov et al.[33] places the band 551.2 cm^{-1} as the most intense (A = 24 relative units) in this region, which strongly supports our assignment. The experimental study of Radchenko et al.[11] provided quantitative measures of intensity of the bands in this region, and it is clear that the band at 550 cm^{-1} is most intense. Barnes et al.[16] also assigned the band 551 cm^{-1} (m) to ν_{27}. The most recent theoretical anharmonic study by Fornaro et al.[59] assigns ν_{27} to a higher observed value of 562 cm^{-1} taken from ref 26, thereby altering the originally correct assignment of the band 551 cm^{-1} to ν_{27}.

To assign ν_{18} and ν_{19}, it is necessary to analyze the shares of the zero-order states and intensities of the predicted resonance triad of ν_{18}, ν_{19}, and $\nu_{28}+\nu_{29}$. The lowest energy state 531.1 cm^{-1} is predominantly (48%) ν_{19}, but it also contains almost equal shares of ν_{18} and $\nu_{28}+\nu_{29}$. The transition to this state is rather weak in the IR spectrum (2.1 km/mol) and in the RS spectrum (3.7 RSU). A close by state at 535.3 cm^{-1} has almost equal shares of ν_{18} and ν_{19} but is more intense in the IR spectrum (7.5 km/mol) and in the RS spectrum (6.3 RSU). Aamouche et al.[35] observed both bands in the RS spectrum at 538 and 528 cm^{-1} and just one band in the IR spectrum at 534 cm^{-1}. Therefore, we assign the RS bands at 538 and 528 cm^{-1} to ν_{18} and ν_{19}, respectively. Convincing evidence for our assignments of ν_{18} and ν_{27} comes from a comparison of their theoretical IR intensities (7.4 and 42.2 km/mol) and the relative intensities of the argon-matrix peaks at 551.2 and 536.4 cm^{-1} (A = 24 and 4 relative units, respectively), as determined by Ivanov et al.[33] The ratios of predicted and observed intensities nearly coincide. There are two more observed weak IR peaks above ν_{27} in an argon matrix at 555 (w) and 559 cm^{-1} (w),[16] which were also found in refs 30 and 33. They may appear as weak components of an FR triad mainly due to the combination state $\nu_{28}+\nu_{29}$. Our assignment is substantially different from the one made in refs 54 and 59.

The last two fundamentals of the A′ symmetry species, ν_{20} and ν_{21}, are resonance free and, according to the predictions (Table 2), are intense in the IR spectrum. The predicted values of 510.8 and 385.6 cm^{-1} agree well with the gas-phase IR values[37] of 512 cm^{-1} (w) and 395 cm^{-1} (w), respectively, and the argon-matrix-isolated values[33] of 516.5 and 391 cm^{-1} (m), respectively.[16]

4.2. Symmetry Block A″. In this symmetry block, all fundamentals, except for ν_{26}, are resonance-free. The assignment of ν_{27} has been already made above because of the A′ peaks that are close to overlapping it.

DOI: 10.1021/acs.jpca.5b03241
J. Phys. Chem. A 2015, 119, 6723−6737

There was much controversy in the literature about the assignments of the close-lying bands for ν_{15}, ν_{16}, and ν_{22}.[10,16,26,54,59] In the two most recent, high-level theoretical interpretations of the spectra for uracil,[54,59] the assignments of all three fundamentals ν_{15}, ν_{16}, and ν_{22} were reconsidered without a discussion. In early works,[10,16] the bands at 846 cm^{-1} (in a nitrogen matrix[10]) and 842 cm^{-1} (vw) (in an argon matrix[16]) were assumed to be due to the ν_{22} fundamental. However, according to theory, this band lies more than 100 cm^{-1} higher. The highest energy A″ fundamental band ν_{22} (955.9 cm^{-1}) has a much lower predicted IR intensity (0.45 km/mol) than the intensity (10.35 km/mol) of the nearby band for ν_{16} (947.5 cm^{-1}). Thus, the band for ν_{22} is probably overshadowed by ν_{16} and was not observed as a separate band in the majority of the experimental studies.[11,16,26,30,33] Their RS intensities are approximately of the same order of magnitude (Table 2), but Barnes et al.[16] observed only one peak with the same frequency 958 cm^{-1} in both the RS and IR spectra. We believe that the RS band at 958 cm^{-1} can be assigned to ν_{22} in agreement with the value used by Fornaro et al.,[59] but further studies are needed to clarify this assignment. In the spectral region below, there is one IR band at 842 cm^{-1} (vw), previously assigned by Barnes et al.[16] to ν_{22}, that is most likely from the combination state $\nu_{25}+\nu_{30}$, the predicted frequency for which is 853.3 cm^{-1} (A = 0.32 km/mol).

The fundamental ν_{23} (803.2 cm^{-1}) is resonance free and has a strong predicted IR intensity of 51.6 km/mol and nil intensity in the RS spectra. The experimental counterpart is 802 cm^{-1} (w) in the gas phase and 804 cm^{-1} (s) in an argon matrix.[16,26,30,33] The next fundamental, ν_{24}, is also readily assignable, even though there is a close-lying band ν_{17} of the A′ symmetry species, because they have the opposite ratio of intensities in IR and RS spectra. The predicted frequency of ν_{24} is 756.1 cm^{-1} with a strong IR intensity (A = 29 km/mol) matches well with the observed gas-phase IR band at 757 cm^{-1} (w)[37] and the same value in an argon matrix at 757 cm^{-1} (s).[16,33] The Raman intensity of ν_{24} is nil, whereas ν_{17} is very intense (see discussion above).

Although the fundamental ν_{25} should be observable in both IR and RS spectra (Table 2), the experimental evidence for it was found only in the IR spectra. The gas-phase IR band at 717 cm^{-1} (w)[37] and the close-lying argon-matrix values[11,16,26,30,33] evidently correspond to ν_{25}.

The Fermi resonance occurs in the region of the fundamental ν_{26}. According to the prediction, this fundamental is heavily mixed with the combination state $\nu_{20}+\nu_{30}$, making a doublet of 648.4 and 651.4 cm^{-1} with strong IR intensities. Both of these transitions are observed experimentally as argon-matrix peaks at 659.5 and 657.3 cm^{-1},[33] whereas in the gas phase only one peak at 660 cm^{-1} (w) was identified.[37] This example is a good illustration of the principal difference between a more traditional description of vibrational spectra in terms of normal modes with one-to-one correspondence between theoretical frequencies and observed bands and an anharmonic picture where a dyad or even a polyad of states can be equally characterized as "fundamental" bands.

There are only close-lying pairs of peaks at 682 and 685 cm^{-1} in an argon matrix[10] and at 682 and 686 cm^{-1} in a nitrogen matrix,[16] which are also observed in the gas phase as 692 cm^{-1} (w). Puzzarini et al.[54] and earlier Ten et al.[52] explained these peaks as combination bands $\nu_{19}+\nu_{30}$ and $\nu_{18}+\nu_{30}$, respectively. Our calculation also predicts the dyad at 675.5 and 678.8 cm^{-1} with predominant shares of $\nu_{19}+\nu_{30}$ and $\nu_{18}+\nu_{30}$, respectively. To explain the intensity borrowing of these distinct bands, it is useful to inspect the Hamiltonian matrix containing relevant couplings. It becomes evident that $\nu_{18}+\nu_{30}$ borrows intensity from both ν_{25} and ν_{26}, whereas $\nu_{19}+\nu_{30}$ is borrowing intensity from ν_{26} only. The coupling coefficients are on the order of 3−6 cm^{-1}. Both combination bands are also coupled through an 11−11 Darling−Dennison resonance that ensures some mixing and repulsion of states.

Although the assignment for ν_{27} was discussed above, ν_{28} is observed both in the gas-phase and an argon-matrix spectra as the peak at 374 cm^{-1} (w),[37] which correlates well with the prediction that this band should be intense in the IR spectrum. The assignment of the two remaining states ν_{29} and ν_{30} are somewhat speculative because they have low intensity and are out of range of most experimental studies. There are essentially two studies that reported transitions suited to ν_{29} and ν_{30} in energy. Fujii et al.[19] studied electronic fluorescence spectra of uracil in a supersonic jet and assigned frequencies at 205 and 149 cm^{-1} to ν_{29} and ν_{30}, respectively. Aamouche et al.[35,36] studied neutron inelastic scattering (NIS) and low-frequency RS spectra of polycrystalline samples of uracil and measured energy levels at 216, 201, 166, 130, and 93 cm^{-1} (NIS) and 132, 100, and 75 cm^{-1} (RS at T = 15 K). These multiple peaks can correspond to solid state vibrations of the unit cell. The calculation predicts the harmonic frequency values of ω_{29} = 159 cm^{-1} and ω_{30} = 140 cm^{-1} with very small anharmonic shifts. It is not possible to make a definitive assignment of ν_{29} and ν_{30} based on available theoretical data, and we accept the assignment made by Fujii et al.[19]

5. CONCLUSIONS

In this work, we have performed a thorough analysis of the abundant experimental data on infrared (IR) and Raman scattering (RS) vibrational spectra of uracil taken from the literature with a state-of-the-art modeling of anharmonic vibrations of this semirigid molecule. We used the numerical-analytic implementation of the second-order canonical Van Vleck perturbation theory (CVPT2) followed by numerical diagonalization of the Hamiltonian matrix containing Fermi (W) and Darling−Dennison (K) resonance coupling coefficients, collectively called CVPT2+*WK*. Our *ab initio* calculation is based on a hybrid potential energy and electro-optical (dipole moment and polarizability) molecular properties surfaces (PES and MPS), represented in the form of Taylor series expansions about the point of equilibrium. Both PES and MPS were calculated using the MP2/cc-pVTZ model for all the properties except for the "best estimated" (CCSD(T)-based) harmonic frequencies, taken from the recent paper of Puzzarini and Barone.[54]

A careful analysis of experimental data and the advanced theoretical calculation improved the average deviation between the predicted and observed fundamental frequencies from 8.4 cm^{-1} (Fornaro et al.[59]) to 4.5 cm^{-1} in this work. Reproduction of observed vibrational frequencies is only part of the outcome expected from a good theoretical model of anharmonic vibrations. It is also necessary to predict relative intensities and separations in Fermi dyads and polyads, as well as IR/RS relative intensities for one-quanta and multiquanta transitions. CVPT2+*WK* is able to model properly multiple resonances and evaluate the IR/RS intensities while taking into account the redistribution of intensities between states in resonance. For the present, the traditional approach (AVPT2+*WK*) will remain

DOI: 10.1021/acs.jpca.5b03241
J. Phys. Chem. A 2015, 119, 6723−6737

as a more economical alternative to CVPT2+*WK* for many applications.

Choi and Miller[47] experimentally measured the absolute IR intensities of ν_1 and ν_2 in helium nanodroplets. We have shown that the accuracy of our theoretical method for these fundamentals is on the order of ∼0.1% for frequencies and on the order of 10−15% for intensities, and the relative ratio of intensities is reproduced with the accuracy of <3%. The quality achieved in reproducing both anharmonic frequencies and IR/RS intensities helps to estimate the expected level of correspondence between the theory and experiment in similar circumstances.

Surprisingly, application of CVPT2 to a semirigid molecule can be performed in a much more automated manner than a traditional harmonic calculation with scaling of the force field in internal coordinate space. With CVPT2, normal modes can be evaluated entirely in Cartesian coordinates and manual assembling of sets of redundant or nonredundant internal coordinates is no longer necessary.

One might argue that wide application of the advanced CVPT2+*WK* algorithm (in comparison with the traditional one, AVPT2+*WK*) is hindered by its algorithmically rather intense nature. In fact, we are not aware of any flawless implementation of AVPT2+*WK*, for the reasons explained above in the body of the article and in our previous publications. Besides, electronic QM calculations that are a lot more sophisticated than CVPT2+*WK* are widespread, are implemented in dozens of software packages, and are used by many groups of researchers. In our opinion, in the case of vibrational studies of molecules up to the size of uracil and when the reliability and precision of calculations matters, CVPT2+*WK* is superior to the traditional AVPT2+*WK*. However, for larger molecules AVPT2+*WK* is an evident leader whereas its implementations can be tested on smaller molecules with the aid of CVPT2+*WK*.

■ ASSOCIATED CONTENT

Supporting Information

The optimized geometry of uracil in the form of G09 Z-matrix, the independent set of internal coordinates, and the harmonic force field in both Cartesian and internal coordinates are provided. The Supporting Information is available free of charge on the ACS Publications website at DOI: 10.1021/acs.jpca.5b03241.

■ AUTHOR INFORMATION

Corresponding Author

*Sergey V. KRASNOSHCHEKOV, Tel.: 7 (495) 939-2950, e-mail: sergeyk@phys.chem.msu.ru.

Notes

The authors declare no competing financial interest.

■ ACKNOWLEDGMENTS

The authors are deeply indebted to Prof. Norman C. Craig for the invaluable help in reading the manuscript and editorial suggestions. We are also grateful to Dr. Rainer Rudert from the University of Ulm for technical assistance. A part of CVPT2 calculations was performed on the Chebyshev Supercomputer in Lomonosov Moscow State University. Financial support by the Dr. B. Mez-Starck Foundation (Germany) is acknowledged.

■ REFERENCES

(1) Császár, A. G.; Fábri, C.; Szidarovszky, T.; Mátyus, E.; Furtenbacher, T.; Czakó, G. The fourth age of quantum chemistry: molecules in motion. *Phys. Chem. Chem. Phys.* **2012**, *14*, 1085−1106.
(2) Angell, C. L. An infrared spectroscopic investigation of nucleic acid constituents. *J. Chem. Soc.* **1961**, 504−515.
(3) Lord, R. C.; Thomas, G. J., Jr. Raman spectral studies of nucleic acids and related molecules-I Ribonucleic acid derivatives. *Spectrochim. Acta, Part A* **1967**, *23*, 2551−2591.
(4) Susi, H.; Ard, J. S. Vibrational spectra of nucleic acid constituents - I: Planar vibrations of uracil. *Spectrochim. Acta, Part A* **1971**, *27*, 1549−1562.
(5) Nowak, M. J.; Szczepaniak, K.; Barski, A.; Shugar, D. Spectroscopic Studies on Vapour Phase Tautomerism of Natural Bases Found in Nucleic Acids. *Z. Naturforsch. C* **1978**, *33*, 876−883.
(6) Peticolas, W. L.; Strommen, D. P.; Lakshminarayanan, V. The use of resonant Raman intensities in refining molecular force fields for Wilson G-F calculations and obtaining excited state molecular geometries. *J. Chem. Phys.* **1980**, *73*, 4185−4191.
(7) Bardi, G.; Bencivenni, L.; Ferro, D.; Martini, B.; Nunziante Cesaro, S.; Teghil, R. Thermodynamic study of the vaporization of uracil. *Thermochim. Acta* **1980**, *40*, 275−282.
(8) Bowman, W. D.; Spiro, T. G. MNDO-MOCIC evaluation of the uracil force field: Application to the interpretation of flavin vibrational spectra. *J. Chem. Phys.* **1980**, *73*, 5482−5492.
(9) Nishimura, Y.; Tsuboi, M.; Kato, S.; Morokuma, K. In-plane vibrational modes in the uracil molecule from an ab initio MO calculation. *J. Am. Chem. Soc.* **1981**, *103*, 1354−1358.
(10) Szczesniak, M.; Nowak, M. J.; Rostkowska, H.; Szczepaniak, K.; Person, W. B.; Shugar, D. Matrix isolation studies of nucleic acid constituents. 1. Infrared spectra of uracil monomers. *J. Am. Chem. Soc.* **1983**, *105*, 5969−5976.
(11) Radchenko, E. D.; Plokhotnichenko, A. M.; Sheina, G. G.; Blagoi, Y. P. Infrared Spectra of Uracil and Thymin in Argon Matrix. *Biofizika* **1983**, *28*, 923−927 (in Russian).
(12) Harsányi, L.; Császár, P. Theoretical Force Fields and Vibrational Spectrum of Uracil by the CNDO/2 Force Method. *Acta Chim. Hungarica* **1983**, *113*, 257−278.
(13) Bandekar, J.; Zundel, G. The role of C═O transition dipole-dipole coupling interaction in uracil. *Spectrochim. Acta, Part A* **1983**, *39*, 337−341.
(14) Bandekar, J.; Zundel, G. Normal coordinate analysis treatment on uracil in solid state. *Spectrochim. Acta, Part A* **1983**, *39*, 343−355.
(15) Chin, S.; Scott, I.; Szczepaniak, K.; Person, W. B. Matrix isolation studies of nucleic acid constituents. 2. Quantitative ab initio prediction of the infrared spectrum of in-plane modes of uracil. *J. Am. Chem. Soc.* **1984**, *106*, 3415−3422.
(16) Barnes, A. J.; Stuckey, M. A.; Le Gall, L. Nucleic acid bases studied by matrix isolation vibrational spectroscopy: Uracil and deuterated uracils. *Spectrochim. Acta, Part A* **1984**, *40*, 419−431.
(17) Maltese, M.; Passerini, S.; Nunziante-Cesaro, S.; Dobos, S.; Harsányi, L. Infrared levels of monomeric uracil in cryogenic matrices. *J. Mol. Struct.* **1984**, *116*, 49−65.
(18) Szczepaniak, K.; Szczesniak, M.; Nowak, M.; Scott, I.; Chin, S.; Person, W. B. Vibrational spectra of uracils: Experimental infrared matrix studies and ab initio quantum-mechanical calculations. *Int. J. Quantum Chem.* **1984**, *18*, 547−569.
(19) Fujii, M.; Tamura, T.; Mikami, N.; Ito, M. Electronic spectra of uracil in a supersonic jet. *Chem. Phys. Lett.* **1986**, *126*, 583−587.
(20) Ghomi, M.; Letellier, R.; Taillandier, E.; Chinsky, L.; Laigle, A.; Turpin, P. Y. Interpretation of the vibrational modes of uracil and its ^{18}O-substituted and thio derivatives studied by resonance Raman spectroscopy. *J. Raman Spectrosc.* **1986**, *17*, 249−255.
(21) Harsányi, L.; Császár, P.; Császár, A.; Boggs, J. E. Interpretation of the vibrational spectra of matrix-isolated uracil from scaled ab initio quantum mechanical force fields. *Int. J. Quantum Chem.* **1986**, *29*, 799−815.

DOI: 10.1021/acs.jpca.5b03241
J. Phys. Chem. A 2015, 119, 6723−6737

(22) Császár, P.; Harsányi, L.; Boggs, J. E. Vibrational Frequencies and Assignments for Some Isotopomers of Uracil Using a Scaled ab Initio Force Field. *Int. J. Quantum Chem.* **1988**, *33*, 1−17.
(23) Brown, R. D.; Godfrey, P. D.; McNaughton, D.; Pierlot, A. P. Microwave spectrum of uracil. *J. Am. Chem. Soc.* **1988**, *110*, 2329−2330.
(24) Wójcik, M. J.; Rostkowska, H.; Szczepaniak, K.; Person, W. B. Vibrational resonances in infrared spectra of uracils. *Spectrochim. Acta, Part A* **1989**, *45*, 499−502.
(25) Nowak, M. J. IR matrix isolation studies of nucleic acid constituents: the spectrum of monomeric thymine. *J. Mol. Struct.* **1989**, *193*, 35−49.
(26) Graindourze, M.; Smets, J.; Zeegers-Huyskens, Th.; Maes, G. Fourier transform-infrared spectroscopic study of uracil derivatives and their hydrogen bonded complexes with proton donors: Part I. Monomer infrared absorptions of uracil and some methylated uracils in argon matrices. *J. Mol. Struct.* **1990**, *222*, 345−364.
(27) Wójcik, M. J. Medium-frequency Raman spectra of crystalline uracil, thymine and their 1-methyl derivatives. *J. Mol. Struct.* **1990**, *219*, 305−310.
(28) Graindourze, M.; Grootaers, T.; Smets, J.; Zeegers-Huyskens, Th.; Maes, G. FT-IR spectroscopic study of uracil derivatives and their hydrogen bonded complexes with proton donors: Part III. Hydrogen bonding of uracils with H2O in argon matrices. *J. Mol. Struct.* **1991**, *243*, 37−60.
(29) Gould, I. R.; Vincent, M. A.; Hillier, I. H. A theoretical study of the infrared spectrum of uracil. *J. Chem. Soc., Perkin Trans. 2* **1992**, 69−71.
(30) Leś, A.; Adamowicz, L.; Nowak, M. J.; Lapinski, L. The infrared spectra of matrix isolated uracil and thymine: An assignment based on new theoretical calculations. *Spectrochim. Acta, Part A* **1992**, *48*, 1385−1395.
(31) Florián, J.; Hrouda, V. Scaled quantum mechanical force fields and vibrational spectra of solid state nucleic acid constituents V: thymine and uracil. *Spectrochim. Acta, Part A* **1993**, *49*, 921−938.
(32) Estrin, D. A.; Paglieri, L.; Corongiu, G. A Density Functional Study of Tautomerism of Uracil and Cytosine. *J. Phys. Chem.* **1994**, *98*, 5653−5660.
(33) Ivanov, A. Yu.; Plokhotnichenko, A. M.; Radchenko, E. D.; Sheina, G. G.; Blagoi, Yu. P. FTIR spectroscopy of uracil derivatives isolated in Kr, Ar and Ne matrices: matrix effect and Fermi resonance. *J. Mol. Struct.: THEOCHEM* **1995**, *372*, 91−100.
(34) Viant, M. R.; Fellers, R. S.; McLaughlin, R. P.; Saykally, R. J. Infrared laser spectroscopy of uracil in a pulsed slit jet. *J. Chem. Phys.* **1995**, *103*, 9502−9505.
(35) Aamouche, A.; Ghomi, M.; Coulombeau, C.; Jobic, H.; Grajcar, L.; Baron, M. H.; Baumruk, V.; Turpin, P. Y.; Henriet, C.; Berthier, G. Neutron Inelastic Scattering, Optical Spectroscopies and Scaled Quantum Mechanical Force Fields for Analyzing the Vibrational Dynamics of Pyrimidine Nucleic Acid Bases. 1. Uracil. *J. Phys. Chem.* **1996**, *100*, 5224−5234.
(36) Aamouche, A.; Berthier, G.; Coulombeau, C.; Flament, J. P.; Ghomi, M.; Henriet, C.; Jobic, H.; Turpin, P. Y. Molecular force fields of uracil and thymine, through neutron inelastic scattering experiments and scaled quantum mechanical calculations. *Chem. Phys.* **1996**, *204*, 353−363.
(37) Colarusso, P.; Zhang, K.; Guo, B.; Bernath, P. F. The infrared spectra of uracil, thymine, and adenine in the gas phase. *Chem. Phys. Lett.* **1997**, *269*, 39−48.
(38) Ilich, P.; Hemann, C. F.; Hille, R. Molecular Vibrations of Solvated Uracil. Ab Initio Reaction Field Calculations and Experiment. *J. Phys. Chem. B* **1997**, *101*, 10923−10938.
(39) Szczepaniak, K.; Person, W. B.; Leszczynski, J.; Kwiatkowski, J. S. Matrix Isolation and DFT Quantum Mechanical Studies of Vibrational Spectra of Uracil and Its Methylated Derivatives. *Polym. J. Chem.* **1998**, *72*, 402−420.
(40) Palafox, M. A.; Rastogi, V. K. Quantum chemical predictions of the vibrational spectra of polyatomic molecules: The uracil molecule and two derivatives. *Spectrochim. Acta, Part A* **2002**, *58*, 411−440.
(41) Palafox, M. A.; Iza, N.; Gil, M. The hydration effect on the uracil frequencies: an experimental and quantum chemical study. *J. Mol. Struct.: THEOCHEM* **2002**, *585*, 69−92.
(42) Giese, B.; McNaughton, D. Surface-Enhanced Raman Spectroscopic Study of Uracil. The Influence of the Surface Substrate, Surface Potential, and pH. *J. Phys. Chem. B* **2002**, *106*, 1461−1470.
(43) Gaigeot, M.-P.; Sprik, M. Ab Initio Molecular Dynamics Computation of the Infrared Spectrum of Aqueous Uracil. *J. Phys. Chem. B* **2003**, *107*, 10344−10358.
(44) Barone, V.; Festa, G.; Grandi, A.; Rega, N.; Sanna, N. Accurate Vibrational Spectra of Large Molecules by Density Functional Computations Beyond the Harmonic Approximation: The Case of Uracil And 2-Thiouracil. *Chem. Phys. Lett.* **2004**, *388*, 279−283.
(45) Él'kin, P. M.; Érman, M. A.; Pulin, O. V. Analysis of Vibrational Spectra of Methyl-Substituted Uracils in the Anharmonic Approximation. *J. Appl. Spectrosc.* **2006**, *73*, 485−491.
(46) V. Vaquero, V.; Sanz, M. E.; López, J. C.; Alonso, J. L. The Structure of Uracil: A Laser Ablation Rotational Study. *J. Phys. Chem. A* **2007**, *111*, 3443−3445.
(47) Choi, M. Y.; Miller, R. E. Infrared Laser Spectroscopy of Uracil and Thymine in Helium Nanodroplets: Vibrational Transition Moment Angle Study. *J. Phys. Chem. A* **2007**, *111*, 2475−2479.
(48) Rasheed, T.; Ahmad, S.; Afzal, S. M.; Rahimullah, K. Anharmonic Vibrational Analysis of Uracil by Ab Initio Hartree-Fock and Density Functional Theory Calculations. *J. Mol. Struct.: THEOCHEM* **2009**, *895*, 18−20.
(49) Biczysko, M.; Panek, P.; Scalmani, G.; Bloino, J.; Barone, V. Harmonic and Anharmonic Vibrational Frequency Calculations with the Double-Hybrid B2PLYP Method: Analytic Second Derivatives and Benchmark Studies. *J. Chem. Theory Comput.* **2010**, *6*, 2115−2125.
(50) Morgado, C. A.; Jurečka, P.; Svozil, D.; Hobza, P.; Šponer, J. Reference MP2/CBS and CCSD(T) Quantum-Chemical Calculations nn Stackedadenine Dimers. Comparison with DFT-D, MP2.5, SCS(MI)-MP2, M06-2X, CBS(SCS-D) and Force Field Descriptions. *Phys. Chem. Chem. Phys.* **2010**, *12*, 3522−3534.
(51) Ten, G. N.; Nechaev, V. V.; Shcherbakov, R. S.; Baranov, V. I. Calculation and Analysis of the Structure and Vibrational Spectra of Uracil Tautomers. *J. Struct. Chem.* **2010**, *51*, 32−39.
(52) Ten, G. N.; Nechaev, V. V.; Krasnoshchekov, S. V. Interpretation of Vibrational IR Spectrum of Uracil Using Anharmonic Calculation of Frequencies and Intensities in Second-Order Perturbation Theory. *Opt. Spectrosc.* **2010**, *108*, 37−44.
(53) Ten, G. N.; Nechaev, V. V.; Pankratov, A. N.; Baranov, V. I. Hydrogen Bonding Effect on the Structure and Vibrational Spectra of Complementary Pairs of Nucleic Acid Bases. I. Adenine-Uracil. *J. Struct. Chem.* **2010**, *51*, 453−462.
(54) Puzzarini, C.; Biczysko, M.; Barone, V. Accurate Anharmonic Vibrational Frequencies for Uracil: The Performance of Composite Schemes and Hybrid CC/DFT Model. *J. Chem. Theory Comput.* **2011**, *7*, 3702−3710.
(55) Puzzarini, C.; Barone, V. Extending the Molecular Size in Accurate Quantum-Chemical Calculations: The Equilibrium Structure and Spectroscopic Properties of Uracil. *Phys. Chem. Chem. Phys.* **2011**, *13*, 7189−7197.
(56) Khaikin, L. S.; Grikina, O. E.; Vogt, N.; Stepanov, N. F. Interpreting the Vibrational Spectra of Uracil Molecules and Their Deuterated Isotopomers Using a Scaled Quantum-Chemical Quadratic Force Field. *Russ. J. Phys. Chem. A* **2012**, *86*, 1855−1861.
(57) Katsyuba, S. A.; Zvereva, E. E.; Burganov, T. I. Is There a Simple Way to Reliable Simulations of Infrared Spectra of Organic Compounds? *J. Phys. Chem. A* **2013**, *117*, 6664−6670.
(58) Vogt, N.; Khaikin, L. S.; Grikina, O. E.; Rykov, A. N. A Benchmark Study of Molecular Structure by Experimental and Theoretical Methods: Equilibrium Structure of Uracil from Gas-Phase Electron Diffraction Data and Coupled-Cluster Calculations. *J. Mol. Struct.* **2013**, *1050*, 114−121.
(59) Fornaro, T.; Biczysko, M.; Monti, S.; Barone, V. Dispersion corrected DFT approaches for anharmonic vibrational frequency

DOI: 10.1021/acs.jpca.5b03241
J. Phys. Chem. A 2015, 119, 6723−6737

calculations: nucleobases and their dimers. *Phys. Chem. Chem. Phys.* **2014**, *16*, 10112−10128.
(60) Császár, A. G.; Demaison, J.; Rudolph, H. D. Equilibrium Structures of Three-, Four-, Five-, Six-, and Seven-Membered Unsaturated N-Containing Heterocycles. *J. Phys. Chem. A* **2015**, *119*, 1731−1746.
(61) Krasnoshchekov, S. V.; Stepanov, N. F. Anharmonic Force Fields and Perturbation Theory in the Interpretation of Vibrational Spectra of Polyatomic Molecules. *Russ. J. Phys. Chem. A* **2008**, *82*, 592−602.
(62) Krasnoshchekov, S. V.; Isayeva, E. V.; Stepanov, N. F. Numerical-Analytic Implementation of the Higher-Order Canonical Van Vleck Perturbation Theory for the Interpretation of Medium-Sized Molecule Vibrational Spectra. *J. Phys. Chem. A* **2012**, *116*, 3691−3709.
(63) Krasnoshchekov, S. V.; Craig, N. C.; Stepanov, N. F. Anharmonic Vibrational Analysis of the Gas-Phase Infrared Spectrum of 1,1-Difluoroethylene Using the Operator Van Vleck Canonical Perturbation Theory. *J. Phys. Chem. A* **2013**, *117*, 3041−3056.
(64) Krasnoshchekov, S. V.; Stepanov, N. F. Polyad Quantum Numbers and Multiple Resonances in Anharmonic Vibrational Studies of Polyatomic Molecules. *J. Chem. Phys.* **2013**, *139*, 184101.
(65) Krasnoshchekov, S. V.; Isayeva, E. V.; Stepanov, N. F. Criteria for First- and Second-Order Vibrational Resonances and Correct Evaluation of the Darling-Dennison Resonance Coefficients Using the Canonical Van Vleck Perturbation Theory. *J. Chem. Phys.* **2014**, *141*, 234114.
(66) Berezin, K. V.; Nechaev, V. V.; Berezin, M. K.; Stepanov, N. F.; Krasnoshchekov, S. V. Theoretical interpretation of the vibrational spectrum of bicyclo[1.1.0]butane in terms of an ab initio anharmonic model. *Opt. Spectrosc.* **2014**, *117*, 366−373.
(67) Krasnoshchekov, S. V.; Stepanov, N. F. Nonempirical Anharmonic Vibrational Perturbation Theory Applied to Biomolecules: Free-Base Porphin. *J. Phys. Chem. A* **2015**, *119*, 1616−1627.
(68) Pulay, P.; Fogarasi, G.; Pongor, G.; Boggs, J. E.; Vargha, A. Combination of Theoretical Ab Initio and Experimental Information to Obtain Reliable Harmonic Force Constants. Scaled Quantum Mechanical (QM) Force Fields for Glyoxal, Acrolein, Butadiene, Formaldehyde, and Ethylene. *J. Am. Chem. Soc.* **1983**, *105*, 7037−7047.
(69) Allen, W. D.; Császár, A. G.; Horner, D. A. The Puckering Inversion Barrier and Vibrational Spectrum of Cyclopentene. A Scaled Quantum Mechanical Force Field Algorithm. *J. Am. Chem. Soc.* **1992**, *114*, 6834−6849.
(70) Scott, A. P.; Radom, L. Harmonic Vibrational Frequencies: An Evaluation of Hartree-Fock, Møller-Plesset, Quadratic Configuration Interaction, Density Functional Theory, and Semi-empirical Scale Factors. *J. Phys. Chem.* **1996**, *100*, 16502−16513.
(71) Yoshida, H.; Ehara, A.; Matsuura, H. Density functional vibrational analysis using wavenumber-linear scale factors. *Chem. Phys. Lett.* **2000**, *325*, 477−483.
(72) Yoshida, H.; Takeda, K.; Okamura, J.; Ehara, A.; Matsuura, H. A New Approach to Vibrational Analysis of Large Molecules by Density Functional Theory: Wavenumber-Linear Scaling Method. *J. Phys. Chem. A* **2002**, *106*, 3580−3586.
(73) Wilson, E. B.; Decius, J. C.; Cross, P. C. *Molecular vibrations: the theory of infrared and Raman vibrational spectra*; McGraw-Hill: New York, 1955.
(74) Nielsen, H. H. The Vibration-Rotation Energies of Molecules. *Rev. Mod. Phys.* **1951**, *23*, 90−136.
(75) Nielsen, H. H. The Vibration-rotation Energies of Molecules and their Spectra in the Infra-red. In *Encyclopedia of Physics*, Vol. *XXXVII/1*; Flügge, S., Ed.; Springer-Verlag: Berlin, 1959.
(76) Mills, I. M. Vibration-Rotation Structure in Asymmetric- and Symmetric-Top Molecules. In *Molecular Spectroscopy: Modern Research*; Rao, K. N., Matthews, C. W., Eds.; Academic Press: New York, 1972.
(77) Califano, S. *Vibrational States*; Wiley: London, 1976.
(78) Papoušek, D.; Aliev, M. R. *Molecular Vibrational/Rotational Spectra*; Academia: Prague, 1982.
(79) Aliev, M. R.; Watson, J. K. G. Higher−Order Effects in the Vibration−Rotation Spectra of Semi-rigid Molecules. In *Molecular Spectroscopy: Modern Research*, Vol. *III*; Rao, K. N., Ed.; Academic Press: NewYork, 1985.
(80) Sarka, K.; Demaison, J. Perturbation Theory, Effective Hamiltonians and Force Constants. In *Computational Molecular Spectroscopy*; Jensen, P., Bunker, P. R., Eds.; John Wiley & Sons Ltd.: New York, 2000.
(81) Harding, L. B.; Ermler, W. C. Polyatomic, Anharmonic, Vibrational-Rotational Analysis. Application to Accurate Ab Initio Results for Formaldehyde. *J. Comput. Chem.* **1985**, *6*, 13−27.
(82) Clabo, D. A., Jr.; Allen, W. D.; Remington, R. B.; Yamaguchi, Y.; Schaefer, H. F., III. A Systematic Study of Molecular Anharmonicity and Vibration-rotation Interaction by Self-Consistent-Field Higher-Derivative Methods. Asymmetric Top Molecules. *Chem. Phys.* **1988**, *123*, 187−239.
(83) Allen, W. D.; Yamaguchi, Y.; Császár, A. G.; Clabo, D. A., Jr.; Remington, R. B.; Schaefer, H. F., III. A Systematic Study of Molecular Vibrational Anharmonicity and Vibration-Rotation Interaction by Self-consistent Field Higher-Derivatives Methods. Linear Polyatomic Molecules. *Chem. Phys.* **1990**, *145*, 427−466.
(84) Green, W. H.; Jayatilaka, D.; Willetts, A.; Amos, R. D.; Handy, N. C. The prediction of spectroscopic properties from quartic corrected force fields: HCCF, HFCO, SiH_3^+. *J. Chem. Phys.* **1990**, *93*, 4965−4981.
(85) Amos, R. D.; Handy, N. C.; Green, W. H.; Jayatilaka, D.; Willetts, A. Anharmonic vibrational properties of CH_2F_2: A Comparison of Theory and Experiment. *J. Chem. Phys.* **1991**, *95*, 8323−8336.
(86) Gaw, J. F.; Willetts, A.; Green, W. H.; Handy. N. C. SPECTRO: A Program for the Derivation of Spectroscopic Constants from Provided Quartic Force Fields and Cubic Dipole Fields In *Advances in Molecular Vibrations and Collision Dynamics*, Vol. *1B*; Bowman, J., Ed.; JAI Press Inc.: Greenwich, CT, 1991; pp 169−185.
(87) Barone, V. Accurate Vibrational Spectra of Large Molecules by Density Functional Computations Beyond the Harmonic Approximation: The Case of Azabenzenes. *J. Phys. Chem. A* **2004**, *108*, 4146−4150.
(88) Barone, V. Vibrational Zero-Point Energies and Thermodynamic Functions Beyond the Harmonic Approximation. *J. Chem. Phys.* **2004**, *120*, 3059−3065.
(89) Barone, V. Anharmonic Vibrational Properties by a Fully Automated Second-Order Perturbative Approach. *J. Chem. Phys.* **2005**, *122*, 014108.
(90) Carbonniere, P.; Lucca, T.; Pouchan, C.; Rega, N.; Barone, V. Vibrational Computations Beyond the Harmonic Approximation: Performances of the B3LYP Density Functional for Semirigid Molecules. *J. Comput. Chem.* **2005**, *26*, 384−388.
(91) Bloino, J.; Biczysko, M.; Barone, V. General Perturbative Approach for Spectroscopy, Thermodynamics, and Kinetics: Methodological Background and Benchmark Studies. *J. Chem. Theory Comput.* **2012**, *8*, 1015−1036.
(92) Davisson, J. L.; Brinkmann, N. R.; Polik, W. F. Accurate and Efficient Calculation of Excited Vibrational States from Quartic Potential Energy Surfaces. *Mol. Phys.* **2012**, *110*, 2587−2598.
(93) Barone, V.; Biczysko, M.; Bloino, J. Fully Anharmonic IR and Raman Spectra of Medium-Size Molecular Systems: Accuracy and Interpretation. *Phys. Chem. Chem. Phys.* **2014**, *16*, 1759−1787.
(94) Hanson, H.; Nielsen, H. H.; Schafer, W. H.; Waggoner, J. Intensities of Rotation Lines in Absorption Bands. *J. Chem. Phys.* **1957**, *27*, 40−43.
(95) Montero, S. Anharmonic Raman Intensities of Overtone, Combination and Difference Bands. *J. Chem. Phys.* **1982**, *77*, 23−29.
(96) Willetts, A.; Handy, N. C.; Green, W. H., Jr.; Jayatilaka, D. Anharmonic Corrections to Vibrational Transition Intensities. *J. Phys. Chem.* **1990**, *94*, 5608−5616.

DOI: 10.1021/acs.jpca.5b03241
J. Phys. Chem. A 2015, 119, 6723−6737

(97) Vásquez, J.; Stanton, J. F. Simple(r) Algebraic Equations for Transition Moments of Fundamental Transitions in Vibrational Second-order Perturbation Theory. *Mol. Phys.* **2006**, *104*, 377−388.
(98) Polavarapu, P. L. Vibrational Optical Activity of Anharmonic Oscillator. *Mol. Phys.* **1996**, *89*, 1503−1510.
(99) Bloino, J.; Barone, V. A Second-Order Perturbation Theory Route to Vibrational Averages and Transition Properties of Molecules: General Formulation and Application to Infrared and Vibrational Circular Dichroism Spectroscopies. *J. Chem. Phys.* **2012**, *136*, 124108.
(100) Vidal, L. N.; Vasquez, P. A. M. CCSD Study of Anharmonic Raman Cross Sections of Fundamental, Overtone, and Combination Transitions. *Int. J. Quantum Chem.* **2012**, *112*, 3205−3215.
(101) Bloino, J. A VPT2 Route to Near-Infrared Spectroscopy: The Role of Mechanical and Electrical Anharmonicity. *J. Phys. Chem. A* **2015**, *119*, 5269.
(102) Darling, B. T.; Dennison, D. M. The water vapor molecule. *Phys. Rev.* **1940**, *57*, 128−139.
(103) Lehmann, K. K. Beyond the x-K relations. Calculation of 1−1 and 2−2 resonance constants with application to HCN and DCN. *Mol. Phys.* **1989**, *66*, 1129−1137.
(104) Martin, J. M. L.; Taylor, P. R. Accurate Ab Initio Quartic Force Field for trans-HNNH and Treatment of Resonance Polyads. *Spectrochim. Acta, Part A* **1997**, *53*, 1039−1050.
(105) Hänninen, V.; Halonen, L. Calculation of Spectroscopic Parameters and Vibrational Overtones of Methanol. *Mol. Phys.* **2003**, *101*, 2907−2916.
(106) Matthews, D. A.; Vásquez, J.; Stanton, J. F. Calculated Stretching Overtone Levels and Darling-Dennison Resonances in Water: a Triumph of Simple Theoretical Approach. *Mol. Phys.* **2007**, *105*, 2659−2666.
(107) Rosnik, A. M.; Polik, W. F. VPT2+K Spectroscopic Constants and Matrix Elements of the Transformed Vibrational Hamiltonian of a Polyatomic Molecule with Resonances Using Van Vleck Perturbation Theory. *Mol. Phys.* **2014**, *112*, 261−300.
(108) Primas, H. Generalized Perturbation Theory in Operator Form. *Rev. Mod. Phys.* **1963**, *35*, 710−712.
(109) Birss, F. W.; Choi, J. H. Contact Transformation and its Application to the Vibrational Hamiltonian. *Phys. Rev. A: At., Mol., Opt. Phys.* **1970**, *2*, 1228−1238.
(110) Tyuterev, V. G.; Perevalov, V. I. Generalized Contact Transformations of a Hamiltonian with a Quasi-Degenerate Zero-Order Approximation. Application to Accidental Vibration-Rotation Resonances in Molecules. *Chem. Phys. Lett.* **1980**, *74*, 494−502.
(111) Makushkin, Yu. S.; Tyuterev, V. G. *Perturbation Methods and Effective Hamiltonians in Molecular Spectroscopy*; Nauka: Novosibirsk, 1984 (in Russian).
(112) Sibert, E. L. Theoretical Studies of Vibrationally Excited Polyatomic Molecules Using Canonical Van Vleck Perturbation Theory. *J. Chem. Phys.* **1988**, *88*, 4378−4390.
(113) Joyeux, M.; Sugny, D. Canonical Perturbation Theory for Highly Excited Dynamics. *Can. J. Phys.* **2002**, *80*, 1459−1480.
(114) Kesharwani, M. K.; Brauer, B.; Martin, J. M. L. Frequency and Zero-Point Vibrational Energy Scale Factors for Double-Hybrid Density Functionals (and Other Selected Methods): Can Anharmonic Force Fields Be Avoided? *J. Phys. Chem. A* **2015**, *119*, 1701−1714.
(115) Martin, J. M. L.; Lee, T. J.; Taylor, P. R.; Francois, J.-P. The Anharmonic Force Field of Ethylene, C_2H_2, by Means of Accurate *Ab Initio* Calculations. *J. Chem. Phys.* **1995**, *103*, 2589−2602.
(116) Kellman, M. E. Approximate Constants of Motion for Vibrational Spectra of Many-Oscillator Systems with Multiple Anharmonic Resonances. *J. Chem. Phys.* **1990**, *93*, 6630−6635.
(117) Kellman, M. E.; Chen, G. Approximate Constants of Motion and Energy Transfer Pathways in Highly Excited Acetylene. *J. Chem. Phys.* **1991**, *95*, 8671−8672.
(118) Kellman, M. E. Algebraic Methods in Spectroscopy. *Annu. Rev. Phys. Chem.* **1995**, *46*, 395−421.
(119) Polik, W. F.; van Ommen, J. R. The Multiresonant Hamiltonian Model and Polyad Quantum Numbers for Highly Excited Vibrational States. In *Highly Excited Molecules: Relaxation, Reaction, and Structure*; Mullin, A. S., Schatz, G. C., Eds.; ACS Symposium Series No. 678; American Chemical Society: Washington, DC, 1997.
(120) Ishikawa, H.; Field, R. W.; Farantos, S. C.; Joyeux, M.; Koput, J.; Beck, C.; Schinke, R. HCP ↔ CPH Isomerization; Caught in the Act. *Annu. Rev. Phys. Chem.* **1999**, *50*, 443−484.
(121) Kellman, M. E.; Tyng, V. The Dance of Molecules: New Dynamical Perspectives on Highly Excited Molecular Vibrations. *Acc. Chem. Res.* **2007**, *40*, 243−250.
(122) Farantos, C.; Schinke, R.; Guo, H.; Joyeux, M. Energy Localization in Molecules, Bifurcation Phenomena, and Their Spectroscopic Signatures: The Global View. *Chem. Rev.* **2009**, *109*, 4248−4271.
(123) Herman, M.; Perry, D. S. Molecular Spectroscopy and Dynamics: A Polyad-Based Perspective. *Phys. Chem. Chem. Phys.* **2013**, *15*, 9970−9993.
(124) Polavarapu, P. L. Ab initio Vibrational Raman and Raman Optical Activity Spectra. *J. Phys. Chem.* **1990**, *94*, 8106−8112.
(125) Krasnoshchekov, S. V.; Nechayev, V. V.; Isayeva, E. V.; Stepanov, N. F. Calculation of Anharmonic Intensities in Vibrational Spectra of Raman Scattering and Full Interpretation of the Vibrational Spectrum of *trans*-1,3-Butadiene. *Moscow Univ. Chem. Bull.* **2010**, *65*, 19−29.
(126) Frisch, M. J.; Trucks, G. W.; Schlegel, H. B.; Scuseria, G. E.; Robb, M. A.; Cheeseman, J. R.; Scalmani, G.; Barone, V.; Mennucci, B.; Petersson, G. A.; et al. *Gaussian 09*, Revision B.01; Gaussian, Inc.: Wallingford, CT, 2010.
(127) Begue, D.; Carbonniere, P.; Pouchan, C. Calculations of Vibrational Energy Levels by Using a Hybrid ab Initio and DFT Quartic Force Field: Application to Acetonitrile. *J. Phys. Chem. A* **2005**, *109*, 4611−4616.
(128) Carbonniere, P.; Lucca, T.; Pouchan, C.; Rega, N.; Barone, V. Vibrational Computations Beyond the Harmonic Approximation: Performances of the B3LYP Density Functional for Semirigid Molecules. *J. Comput. Chem.* **2005**, *26*, 384−388.

DOI: 10.1021/acs.jpca.5b03241
J. Phys. Chem. A 2015, 119, 6723−6737